Ecological Complexity 31 (2017) 149–164

Contents lists available at ScienceDirect

Ecological Complexity

journal homepage: www.elsevier.com/locate/ecocom

Original Research Article

On dynamics underlying variance of mass balance estimation in Chilean glaciers

M. Stehlík[a,b,*], P. Hermann[a], S. Torres[c], J. Kiseľák[a,d], A. Rivera[e,f]

[a] Department of Applied Statistics and Linz Institute of Technology, Johannes Kepler University Linz, Altenbergerstraße 69, 4040 Linz, Austria
[b] Institute of Statistics, University of Valparaíso, Blanco 951, Valparaíso, Region de Valparaíso, Chile
[c] Departamento de Matemática, Universidad Técnica Federico Santa María, Casilla 110-V, Valparaíso, Chile
[d] Institute of Mathematics, P.J. Šafárik Univesity in Košice, Slovakia
[e] Laboratorio de Glaciología, Centro de Estudios Científicos (CECs), Arturo Prat 514, Valdivia, Chile
[f] Departamento de Geografía, Universidad de Chile, Marcoleta 250, Santiago, Chile

ARTICLE INFO

Article history:
Received 31 March 2017
Received in revised form 16 June 2017
Accepted 22 June 2017
Available online 7 July 2017

MSC:
Primary 62K05
62K15
Secondary 62M30

Keywords:
D-optimality
Variance
Dynamical system
Blow-up
Glaciers
Mass balance

ABSTRACT

Mass balance of a glacier is an accepted measure of how much mass a glacier gains or loses. In theory, it is typically computed by integral functional and empirically, it is approximated by arithmetic mean. However, the variability of such an approach was not studied satisfactory yet. In this paper we provide a dynamical system of mass balance measurements under the constrains of 2nd order model with exponentially decreasing covariance. We also provide locations of optimal measurements, so called designs. We study Ornstein–Uhlenbeck (OU) processes and sheets with linear drifts and introduce K optimal designs in the correlated processes setup. We provide a thorough comparison of equidistant, Latin Hypercube Samples (LHS), and factorial designs for D- and K-optimality as well as the variance. We show differences between these criteria and discuss the role of equidistant designs for the correlated process. In particular, applications to estimation of mass balance of Olivares Alfa and Beta glaciers in Chile is investigated showing that simple application of full raster design and kriging based on inter- and extrapolation of points can lead to increased variance. We also show how the removal of certain measurement points may increase the quality of the melting assessment while decreasing costs. Blow-ups of solutions of dynamical systems underline the empirically observed fact that in a homogenous glaciers around 11 well-positioned stakes suffices for mass balance measurement.

1. Introduction

Glacier mass balance is an important measure of the glacier health, since accounts for the mass gains and losses during a specific period of time, normally a hydrological or calendar year (Rivera et al., 2016). We will focus in the glaciological method (Cogley et al., 2012), here the mass balance is measured at stakes or poles' networks installed on the glacier surface, whose distribution depends on altitude, slope, topography, and other parameters. In many cases, the distribution is skewed or seriously limited by accessibility (mainly due to crevasses) or logistical constrains. These measurements are ideally done at monthly frequency, but accessibility or budget limitations reduce the number of surveys, sometimes to a very minimum of two per year, one in the accumulation season peak and another in the ablation season maximum. The stakes height above the snow/ice surface at the beginning of the mass balance year (normally at the end of the ablation season), is therefore compared to successive measurements along the year, when snow/ice density must be also determined in order to convert vertical heights into water equivalent volumes (Cuffey and Paterson, 2010). The discrete mass balance data must be integrated over the entire glacier surface by applying geo-spatial interpolation methods or simply by computing the arithmetic mean of measurements (Cogley et al., 2012).

The effective sample size has been addressed previously in (Cogley, 1999), where the analysis of multiple time series of point mass balance measurements have shown that correlation decreases along differences in elevation between the points. A

* Corresponding author at: Department of Applied Statistics and Linz Institute of Technology, Johannes Kepler University Linz, Altenbergerstraße 69, 4040 Linz, Austria.
E-mail addresses: mlnstehlik@gmail.com (M. Stehlík), philipp.hermann@jku.at (P. Hermann), sebastian.torresle@alumnos.usm.cl (S. Torres), jozef.kiselak@gmail.com (J. Kiseľák), arivera@cecs.cl (A. Rivera).

http://dx.doi.org/10.1016/j.ecocom.2017.06.008
1476-945X/

similar conclusion is obtained in Fountain and Vecchia (1999), where the dominant effect of the gradient of mass balance with altitude was shown to be more relevant than transverse variations. Hence, the number of mass balance measurements required to determine the mass balance appears to be scale invariant for small glaciers ($<10\,km^2$) with five to ten stakes being enough.

In this paper we define an underlying dynamical system, thus putting measurement locations and underlying parameters into dynamical relation. Such dynamical systems can appear naturally because of various modelling modalities (see Stehlík et al., 2016, 2017). Based on this background we discuss the statistical optimality of stakes distributed over the glacier. A problem which arises is that neither locations nor measurements themselves are independent. This is why we provide a comparison between monotonic and space-filling designs, introduced in the case of Ornstein–Uhlenbeck (OU) sheets in Baran et al. (2013); Baran and Stehlík (2015). We consider both, D- and K-optimality and minimization of variance of arithmetic mean. Practically, we study Smit's paradox (Smit, 1961) for planar Ornstein Uhlenbeck process, so called OU sheet.

In the next section we show different designs strategies, then in Section 3, we consider OU processes and OU sheet. We continue with Section 4 where we provide a motivating example on mass balance for glaciers Olivares Alpha and Beta in Chile. Some results follow in Section 5 where the simulation on defined optimal design criteria allows us to compare different design strategies. Section 6 contains the unpleasant increment of variance after using kriging methods for the estimation of the mass balance. Moreover, the variance changes after the removal of stakes, even showing a decrease of it under a particular covariance structure. Finally, Section 7 provides a dynamical system and blow-ups in order to technically explain interrelations between parameters and design points. We show, that under some generic circumstances variance of mass balance estimator can grow with the number of stakes.

2. Optimal design under correlated errors

In many situations we can meet problems of unavoidable increase of variance (this can be related to Smit's work Smit, 1961) when using additional interpolation or extrapolation by simple kriging. Hence, more sophisticated designs than usage of full rasterization of the grid, namely equidistant, factorial, Latin Hypercube Samples under S-optimality (LHS^*) and Latin Hypercube Samples optimal with respect to Euclidean distances (LHS^+) designs are compared with respect to D- and K-optimality as well as the variance. Therefore, mass balance estimation of glaciers Olivares Alpha and Beta, important meltwater contributors to the Maipo River in Santiago, requires proper data sampling techniques. To construct such techniques, we need to deal with optimal design strategies.

The determination of optimal designs for models with correlated errors is substantially more difficult and for this reason not sufficiently developed. A stochastic process with parameterized mean and covariance is observed on a compact set. The information obtained from observations is measured through the information functional (defined on the Fisher information matrix (FIM)). We focus on efficient designs for parameters of correlated processes and discuss the role of equidistant designs for correlated processes. Such designs have been proven to be optimal for parameters of trend of stationary Ornstein–Uhlenbeck process (see Kiselák and Stehlík, 2008). For such a process a study of small samples and asymptotical comparisons of the efficiencies of equidistant designs was provided whilst taking both the parameters of trend as well as the parameters of covariance into account. If only trend parameters are of interest, the designs covering more or less uniformly the whole design space will rather be efficient when correlation decreases exponentially (see Kiselák and Stehlík, 2008). Some other issues on designs for spatial processes, i.e. identifiablity and existence of optimal designs, are given in Dette et al. (2008); Müller and Stehlík (2009); Stehlík et al. (2008). The role of heteroscedasticity is studied in Boukouvalas et al. (2014).

Exact K-optimal designs have been firstly introduced by Ye and Zhou (2013) in the setup of polynomial regression models and were later extended in Rempel and Zhou (2014). Both of these setups consider cases having independent errors. K-optimality is a new design criterion for the construction of regression designs, based on the condition number of the information matrix. Thus, K-optimal design minimizes the condition number $\kappa(M)$ of Fisher information matrix M, i.e.

$$\kappa(M) = \frac{\lambda_1(M)}{\lambda_p(M)},$$

if $\lambda_p(M) > 0$ and ∞ otherwise. Here, $\lambda_1(M)$ and $\lambda_p(M)$ are the largest and the smallest eigenvalues, respectively.

Multicollinearity is a common problem when estimating linear or generalized linear models. It occurs when there are high correlations among the predictor variables, leading to unreliable and unstable estimates of regression coefficients. However, many data analysts do not realize that there are several situations in which multicollinearity can be safely ignored, and we hope that K-optimal design is a helpful tool in this direction (see Baran, S., K-optimal designs for parameters of shifted Ornstein-Uhlenbeck processes andsheets. J. Stat. Plan. Inference 186 (2017), 28–41).

3. Ornstein–Uhlenbeck process and sheet

Consider the stochastic process

$$Y(s) = \alpha_1 + \alpha_2 s + \varepsilon(s), \tag{1}$$

where $C(\varepsilon(s), \varepsilon(t)) = \exp(-r|s-t|)$. For model (1) the Fisher information matrix $M_\theta(n)$ on the unknown parameter vector $\theta = (\alpha_1, \alpha_2)$ based on observations $\{Y(s_i),\ i = 1, 2, \ldots, n\}$, $n \geq 2$, equals

$$M_\theta(n) = H(n)C(n)^{-1}H(n)^\top, \quad \text{where} \quad H(n) : = \begin{pmatrix} 1 & 1 & \cdots & 1 \\ s_1 & s_2 & \cdots & s_n \end{pmatrix},$$

and $C(n)$ is the covariance matrix of the observations (see Pázman, 2007; Xia et al., 2006). On the other hand, consider now the stationary process

$$Y(s,t) = \theta + \varepsilon(s,t) \tag{2}$$

with design points taken from a compact design space $\mathcal{X} = [a_1, b_1] \times [a_2, b_2]$, where $b_1 > a_1$ and $b_2 > a_2$ and $\varepsilon(s,t), s,t \in \mathbb{R}$, is a stationary Ornstein–Uhlenbeck sheet, that is a zero mean Gaussian process with covariance structure

$$\mathrm{E}\,\varepsilon(s_1,t_1)\varepsilon(s_2,t_2) = \frac{\tilde{\sigma}^2}{4\alpha\beta}\exp(-\alpha|t_1 - t_2| - \beta|s_1 - s_2|), \tag{3}$$

where $\alpha > 0, \beta > 0, \tilde{\sigma} > 0$. We remark that $\varepsilon(s,\ t)$ can also be represented as

$$\varepsilon(s,t) = \frac{\tilde{\sigma}}{2\sqrt{\alpha\beta}}\mathrm{e}^{-\alpha t - \beta s}\mathcal{W}(\mathrm{e}^{2\alpha t}, \mathrm{e}^{2\beta s}),$$

where $\mathcal{W}(s,t), s,t \in \mathbb{R}$, is a standard Brownian sheet (Baran et al., 2013). Under this setup we compute Fisher information (FIM) for four designs defined in Section 2. Eq. (4) computes FIM for equidistant design points on the diagonal of a square $[0,1] \times [0,1]$ (also equidistant on diagonal line (EDL) hereafter). Eq. (5) calculates FIM for factorial design with points in $[0,\ 1] \times [0,\ 1]$. Fisher information matrix calculation for the LHS designs (both

LHS^* and LHS^+) is based on Eq. (5). Eqs. (4) and (5) show the differences in the computation of $M_\theta(n)$, representing FIM of θ with respect to n, the number of design points:

$$M_\theta(n) = 1 + \sum_{i=1}^{n-1} \frac{1-q_i}{1+q_i}, \qquad \text{where } q_i = \exp(-\alpha d_i - \beta\delta_i) \tag{4}$$

$$M_\theta(n) = \mathbf{1}_n C^{-1}(n,r)\mathbf{1}_n, \qquad \text{with covariance defined by (3)} \tag{5}$$

and $\alpha > 0, \beta > 0, \tilde{\sigma} > 0$. Moreover, we have $d_i = |t_i - t_{i+1}|$ and $\delta_i = |s_i - s_{i+1}|$. In the following computations, parameters α and β were set 1 and $\tilde{\sigma} = 2$. Hence, the fraction of the covariance structure in Eq. (3) equals to one.

4. Glaciological context

The Olivares basin (33°10′ S – 70°08′ W) is the most glaciated area of the Maipo River where the Chilean capital Santiago is located. The Olivares basin has approximately 77 km^2 of ice distributed among 148 glaciers. The basin has experienced a strong area shrinkage in recent decades, with about 25 km^2 of area lost since 1955. In the upper part of this basin there are several glaciers, including Olivares Alfa (3.8 km^2 in 2015, Fig. 1 left) and Beta (7.4 km^2 in 2015, Fig. 1 right). These two glaciers were joining together in 1955, but are now separated by a number of bare rocks and moraine terrains. These glaciers have been studied in detail by CECs (Center for Scientific Studies, Valdivia, Chile) since they are important meltwater contributors to the Maipo River. The mass balance program initiated in 2012 shows a strong negative value for both glaciers in the last two years. This mass balance program is important for understanding the glacier responses to annual variations in the meteorological conditions affecting the region. This issue is a focus of increasing concern in Chile, since in the last 7 years, the central Andes of Chile have experienced one of the most prolonged and driest periods in the historical record. All noted information underpins the national relevance of the zone of glaciers Olivares Alfa and Olivares Beta. Therefore, this natural phenomena has to be studied in depth and with major care.

5. Simulations

5.1. Comparison with respect to D- and K-optimality criterion

The following simulation study compares efficiencies of D- and K-optimality criterion for the models with constant and linear trend. In this regard, we compare the four designs equidistant, factorial, LHS with respect to S-optimality, denoted as LHS^* and improved-LHS based on optimal Euclidean distances, abbreviated via LHS^+. Fig. 2 provides visualizations[1] of both LHS designs for $n = 6, 7, 10, 15$. Note that for factorial design we only consider $n = 4$ observations in this paper, which are located at the edges of the $[0, 1] \times [0, 1]$ square, yielding {(0,0), (0,1), (1,0), (1,1)}. Equidistant design results in points with equal distances on the diagonal of the aforenamed square.

For the sake of averaging out present variation in the simulation, 1000 replicates are computed and the harmonic mean (due to its robustness property in comparison to e.g. arithmetic mean) of efficiencies is computed. The estimated efficiencies are summarized in Table 1 for constant trend with $\alpha = \beta = \tilde{\sigma} = 1$. Efficiencies were computed as the values of D- and K-optimality criteria were divided by their corresponding maximum and minimum values per design points, respectively. Notice that their absolute values are provided in the tables. More precisely, we consider efficiencies of K-optimality as the inverse of the values divided by their minimum values. As the header of the table shows, the first column displays the number of generated design points and the second one efficiencies with respect to FIM with equidistant on diagonal line design points. In the third column efficiency resulting from factorial design is shown and the lasttwo columns present the results for the two different optimizing approaches of Latin Hypercube Samples designs. The same structure as for D-criterion in columns 2–5 is provided for K-criterion in columns 6–9.

Table 1 shows that factorial design (constant based on $n = 4$) outperforms its opponents for less than inclusive 20 observations under D-criterion. However, it is shown that LHS under S-optimality has higher efficiency based on the harmonic mean of

[1] These were performed with the functions `geneticLHS` and `improvedLHS` of the R-package `lhs` (Carnell, 2012).

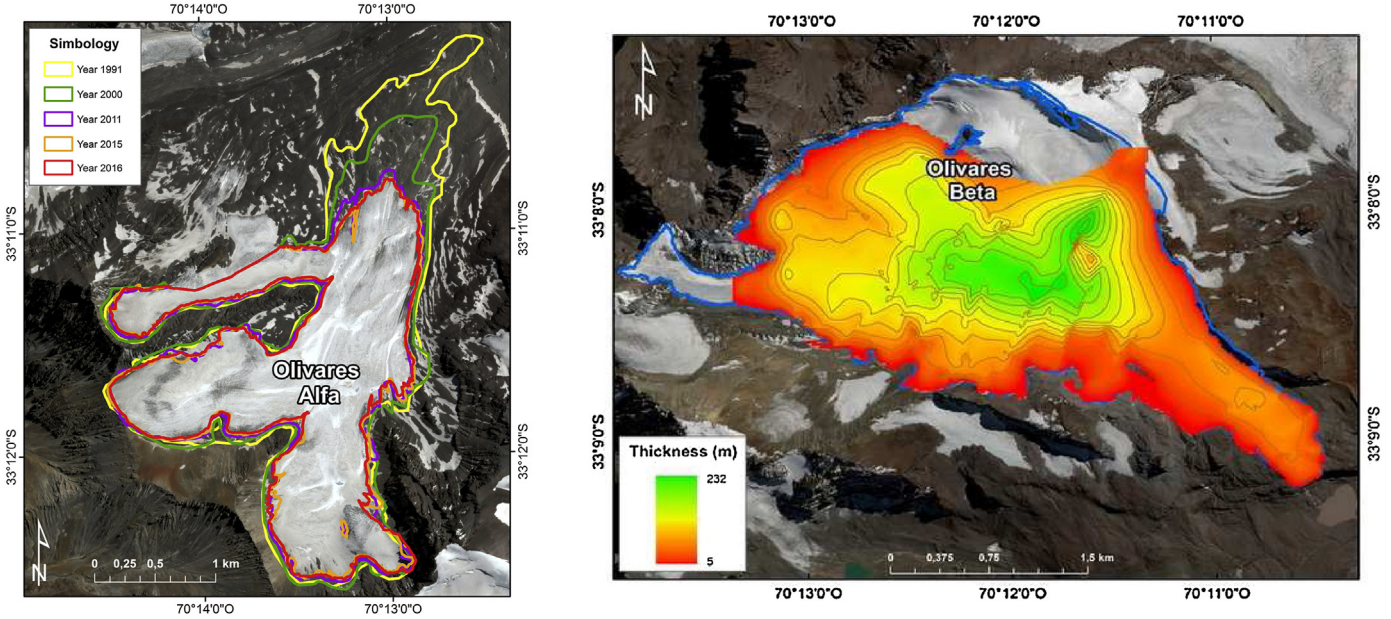

Fig. 1. Illustrations of glaciers Olivares Alfa (left) and Beta (right).

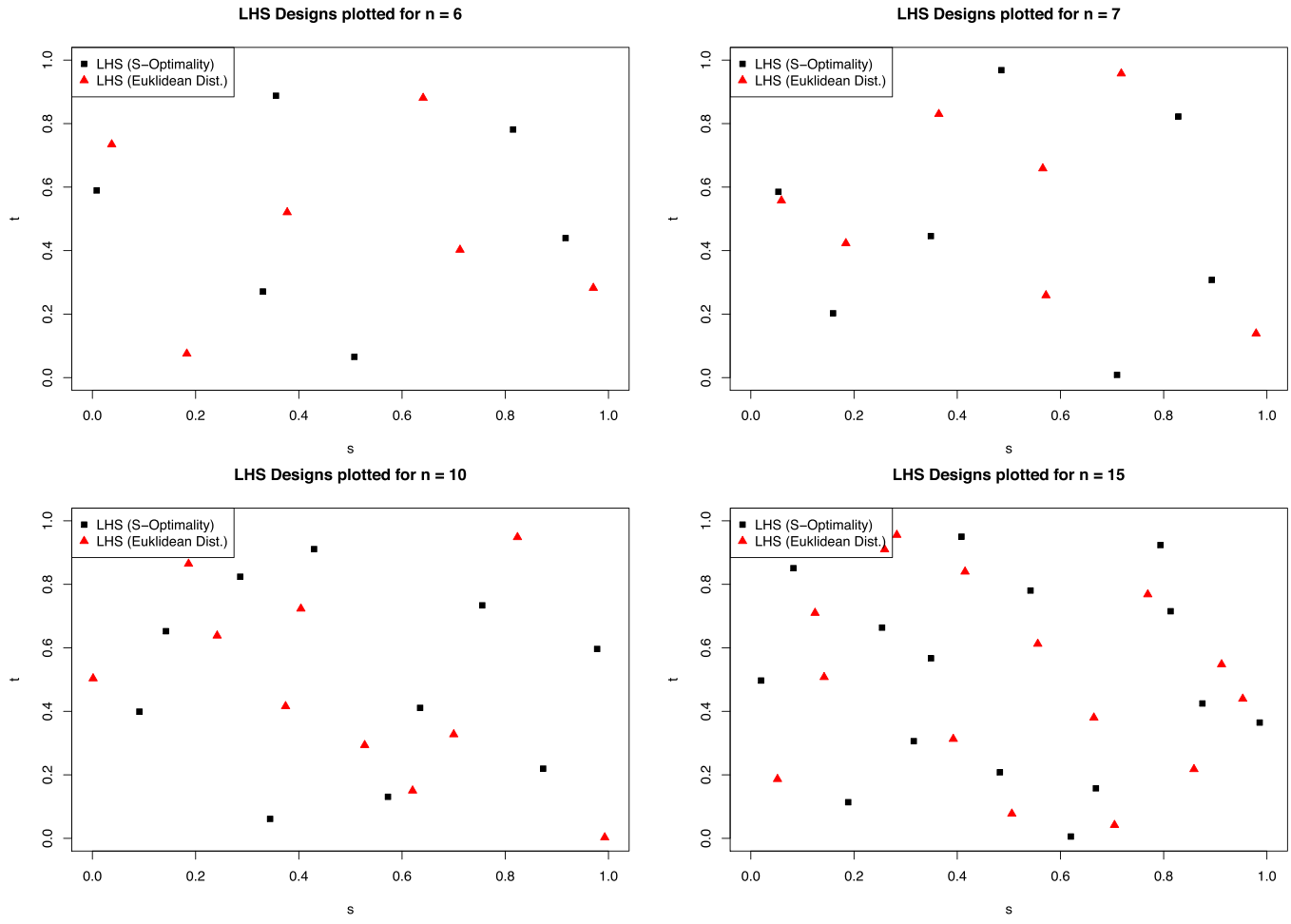

Fig. 2. Visualizations of LHS with respect to S-optimality (black squares) and LHS based on optimal Euclidean distances (red triangles) for $n = 6$ (topleft), 7 (topright), 10 (bottomleft), and 15 (bottomright). (For interpretation of the references to color in this figure legend, the reader is referred to the web version of the article.)

Table 1
Harmonic means of efficiencies of D-criterion and of K-criterion for equidistant, factorial, LHS* (S-optimality) and LHS+ (improved LHS as optimal with respect to Euclidean distances) under constant trend.

n	D-criterion				K-criterion			
	Equidistant	Factorial	LHS*	LHS+	Equidistant	Factorial	LHS*	LHS+
2	0.0282	1.0000	0.0049	0.0081	0.1793	1.0000	0.4023	0.4092
3	0.0144	1.0000	0.0844	0.0771	1.0000	9.5634	6.9041	6.5843
4	0.0387	1.0000	0.0280	0.2367	1.0000	3.3019	3.0389	2.5691
5	0.0542	1.0000	0.1949	0.1093	1.0000	2.2344	2.2830	2.0234
6	0.0650	1.0000	0.1217	0.0890	1.0000	1.7943	1.9345	1.6759
7	0.0730	1.0000	0.2156	0.1259	1.0000	1.5546	1.7311	1.4489
8	0.0791	1.0000	0.2464	0.1417	1.0000	1.4040	1.5578	1.4037
9	0.0839	1.0000	0.2969	0.0496	1.0000	1.3006	1.4310	1.3086
10	0.0878	1.0000	0.3083	0.4260	1.0000	1.2253	1.3243	1.2282
15	0.0997	1.0000	0.5540	0.4012	1.0000	1.0316	0.9822	1.0189
20	0.1058	1.0000	0.7841	0.4871	1.0000	0.9496	0.7776	0.8708
30	0.0924	0.8250	1.0000	0.7096	1.0000	0.8756	0.5621	0.6612
40	0.0689	0.5985	1.0000	0.7306	1.0000	0.8413	0.4299	0.5259
50	0.0567	0.4839	1.0000	0.7483	1.0000	0.8215	0.3557	0.4384
75	0.0381	0.3181	1.0000	0.7583	1.0000	0.7960	0.2439	0.3079
100	0.0286	0.2365	1.0000	0.7677	1.0000	0.7835	0.1865	0.2368

1000 experiments for at least 30 design points. In contrast to that, equidistant design performs best under K-criterion except for having two observations, where factorial design is preferable (recall that factorial design always bases on 4 observations).

Fig. 3 provides the development of the harmonic means of relative efficiencies of D- (left) and K-optimality criteria (right) under constant (top row) and linear (bottom row) trend. This enables to graphically compare the performances between the two models with respect to the number of design points as well as between the analyzed designs. Strong variation in the efficiency of both LHS designs is apparent for less than 20 observations. However, LHS under S-optimality performs uniformly better than

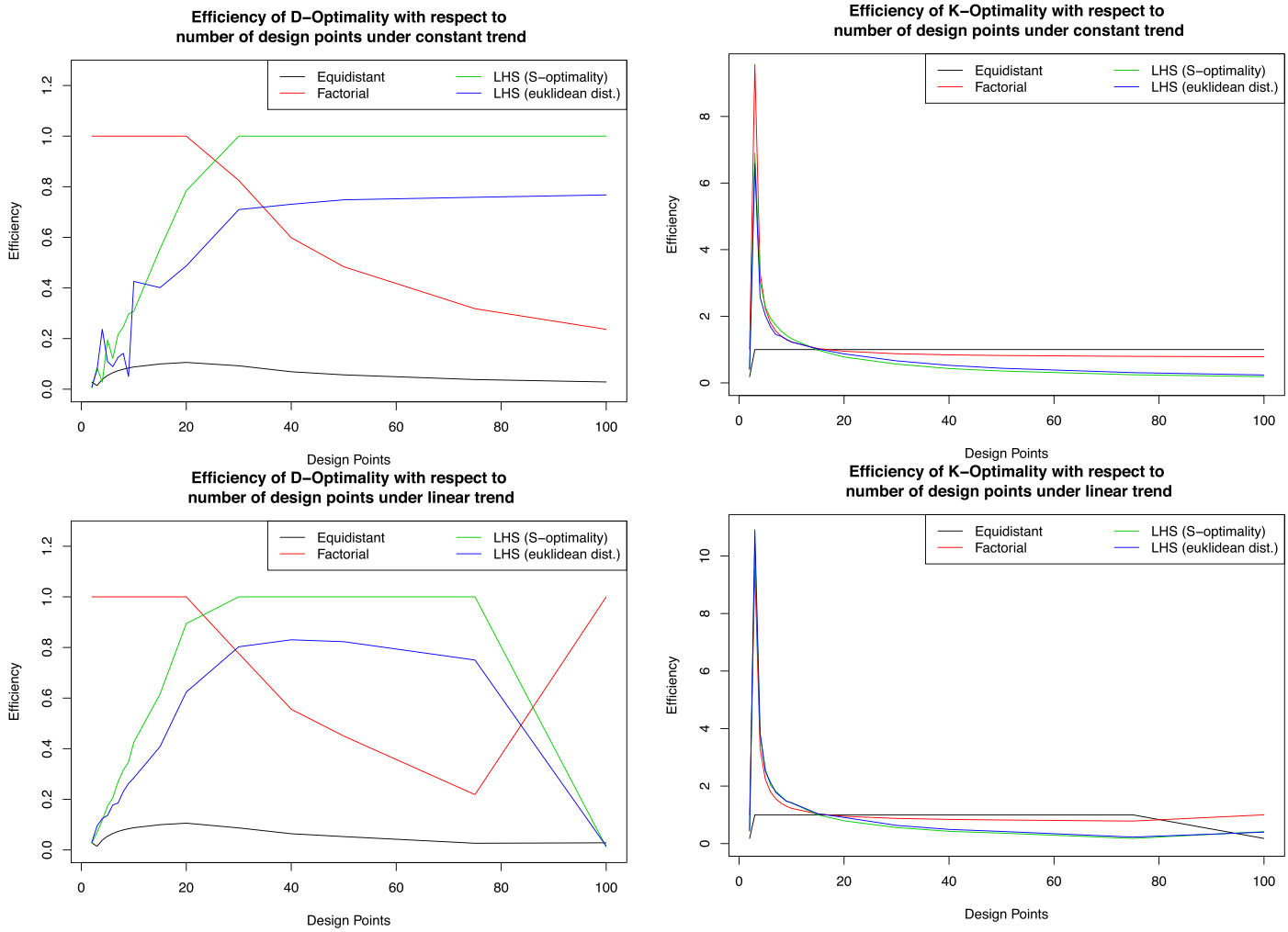

Fig. 3. Relative efficiencies for D- (left) and K-optimality criteria (right) under given designs and various number of design points under constant (top row) and linear (bottom row) trend.

LHS under optimal Euclidean distances when having more than 15 observations with respect to D-optimality.

Table 2 compares the performance of the efficiency for the model under a linear trend. Therein, one can observe the same performance under D-optimality criterion as in the constant case, except for the case of 100 observations where factorial design is more efficient. Another difference to the results for the model under constant trend is the highest efficiency of factorial design for

Table 2
Harmonic means of efficiencies of D-criterion (column 2-5) and of K-criterion (column 6–9) for equidistant, factorial, LHS* (S-optimality) and LHS$^+$ (improved LHS as optimal with respect to Euclidean distances) under linear trend.

n	D-criterion				K-criterion			
	Equidistant	Factorial	LHS*	LHS$^+$	Equidistant	Factorial	LHS*	LHS$^+$
2	0.0282	1.0000	0.0275	0.0307	0.1793	1.0000	0.4630	0.4327
3	0.0144	1.0000	0.0700	0.0947	1.0000	9.5634	10.4295	10.9103
4	0.0387	1.0000	0.1171	0.1244	1.0000	3.3019	3.7605	3.8640
5	0.0542	1.0000	0.1730	0.1361	1.0000	2.2344	2.5829	2.5183
6	0.0650	1.0000	0.2060	0.1775	1.0000	1.7943	2.0226	2.1212
7	0.0730	1.0000	0.2689	0.1854	1.0000	1.5546	1.8217	1.7789
8	0.0791	1.0000	0.3154	0.2305	1.0000	1.4040	1.6533	1.6230
9	0.0839	1.0000	0.3473	0.2625	1.0000	1.3006	1.4798	1.4766
10	0.0878	1.0000	0.4254	0.2846	1.0000	1.2253	1.4156	1.4197
15	0.0997	1.0000	0.6155	0.4083	1.0000	1.0316	0.9995	1.0388
20	0.1058	1.0000	0.8943	0.6239	1.0000	0.9496	0.7918	0.9105
30	0.0870	0.7763	1.0000	0.8027	1.0000	0.8756	0.5584	0.6333
40	0.0640	0.5558	1.0000	0.8302	1.0000	0.8413	0.4271	0.4931
50	0.0527	0.4501	1.0000	0.8229	1.0000	0.8215	0.3644	0.4235
75	0.0264	0.2185	1.0000	0.7504	1.0000	0.7835	0.1817	0.2263
100	0.0282	1.0000	0.0121	0.0153	0.1793	1.0000	0.4156	0.3983

Table 3
Ratio of efficiencies of D-criterion (column 2–5) and of K-criterion (column 6–9) for equidistant, factorial, LHS* (S-optimality) and LHS+ (improved LHS as optimal with respect to Euclidean distances).

n	D-criterion				K-criterion			
	Equidistant	Factorial	LHS*	LHS+	Equidistant	Factorial	LHS*	LHS+
2	1.0000	1.0000	5.5870	3.8048	1.0000	1.0000	1.1508	1.0576
3	1.0000	1.0000	0.8285	1.2275	1.0000	1.0000	1.5106	1.6570
4	1.0000	1.0000	4.1903	0.5255	1.0000	1.0000	1.2375	1.5040
5	1.0000	1.0000	0.8879	1.2453	1.0000	1.0000	1.1314	1.2446
6	1.0000	1.0000	1.6926	1.9957	1.0000	1.0000	1.0456	1.2657
7	1.0000	1.0000	1.2473	1.4724	1.0000	1.0000	1.0523	1.2278
8	1.0000	1.0000	1.2797	1.6263	1.0000	1.0000	1.0613	1.1562
9	1.0000	1.0000	1.1697	5.2907	1.0000	1.0000	1.0341	1.1284
10	1.0000	1.0000	1.3799	0.6681	1.0000	1.0000	1.0690	1.1560
15	1.0000	1.0000	1.1110	1.0175	1.0000	1.0000	1.0176	1.0195
20	1.0000	1.0000	1.1406	1.2808	1.0000	1.0000	1.0183	1.0456
30	0.9410	0.9410	1.0000	1.1312	1.0000	1.0000	0.9934	0.9577
40	0.9285	0.9285	1.0000	1.1363	1.0000	1.0000	0.9935	0.9376
50	0.9300	0.9300	1.0000	1.0996	1.0000	1.0000	1.0246	0.9660
75	0.6942	0.6868	1.0000	0.9896	1.0000	0.9844	0.7446	0.7351
100	0.9859	4.2276	0.0121	0.0199	0.1793	1.2763	2.2276	1.6820

100 observations under K-criterion. Recall that the model with constant trend identifies equidistant design to be most efficient for these design points.

For the sake of comparing the model under constant and linear trend, we computed relative ratios (linear/constant) in Table 3, of the relative efficiencies based on the harmonic means of 1000 replicates. Note that values equal to one show equality of the two models. However, ratios smaller than 1 indicate the linear trend model as less efficient and for ratios larger than 1 vice versa. Naturally, the closer the ratio is to zero and the higher the value is, linear trend model is much more and much less efficient, respectively.

Table 4
Arithmetic mean of efficiency for OU-sheet of FIM for different number of design points of equidistant on diagonal line, factorial, LHS* (S-optimality) and LHS+ (improved LHS as optimal with respect to Euclidean distances)

n	EDL	Factorial	LHS*	LHS+
2	0.8240	1.0000	0.6818	0.6780
3	0.9001	1.0000	0.7680	0.7663
4	0.9190	1.0000	0.8103	0.8140
5	0.9260	1.0000	0.8320	0.8405
6	0.9294	1.0000	0.8488	0.8607
7	0.9313	1.0000	0.8703	0.8780
8	0.9324	1.0000	0.8834	0.8904
9	0.9331	1.0000	0.8938	0.9011
10	0.9336	1.0000	0.9029	0.9096
15	0.9348	1.0000	0.9327	0.9400
20	0.9351	1.0000	0.9505	0.9597
30	0.9354	1.0000	0.9704	0.9815
40	0.9354	1.0000	0.9830	0.9940
50	0.9331	0.9975	0.9891	1.0000
75	0.9221	0.9857	0.9906	1.0000
100	0.9158	0.9789	0.9919	1.0000

5.2. Design optimality with an OU sheet

According arithmetic means for efficiencies (calculated as previously) of OU sheet with respect to FIM for several design points are listed in Table 4, (with the same structure as the previous tables) based on 1000 replicates. Certainly, $M_\theta(n)$ increases with larger number of design points and different magnitudes of increases between the approaches are obtained (values not reported here). Table 4 follows the same structure as the previous tables. Fisher information for the factorial design equals to 3.9147 for every n, because this computation can only be performed for the four possible points. Further computations of this design are impossible in this setup without additional conditions. Table 4 shows that LHS designs have higher efficiency beginning with at least 50 (75 in the case of optimal Euclidean distances) observations. Thereby, LHS under S-optimality is preferable over LHS optimal with respect to Euclidean distances.

Fig. 4 contains two plots showing the development of efficiency with respect to FIM taking both, the number of design points and

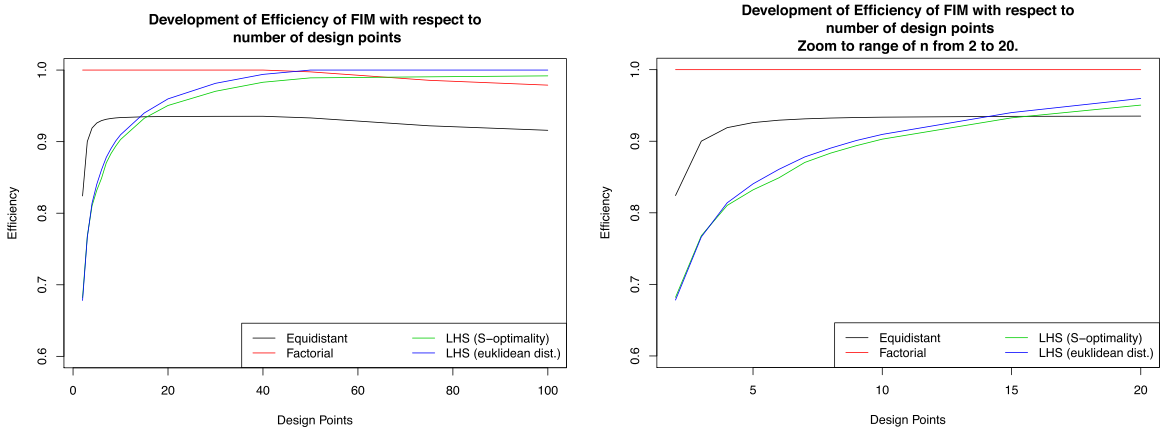

Fig. 4. Overall development of efficiency of FIM for number of design points (left) and a zoom to $2 \leq n \leq 20$ (right).

the four introduced designs into account. The left plot shows that factorial design leads to highest efficiency with less than 40 design points. The calculated arithmetic means of efficiency for the two LHS designs overtake EDL design beginning with approximately 15 observations. FIM for equidistant on diagonal line design is increasing slowly (from $n = 10$ to $n = 100$, $\Delta = 0.5901$; exact values not reported here). Hence, the higher the number of observations the larger is the difference in terms of FIM compared to the two LHS approaches. We can also observe that LHS with optimal Euclidean distances performs better than factorial design with n higher than 40. In contrast to that, LHS under S-optimality condition shows higher FIM only for $n \geq 75$. On the right hand side of Fig. 4 we highlight the development of FIM when considering designs from 2 to 20 observations. Thereby, optimizing LHS with respect to Euclidean distances results in higher Fisher information compared to its counterpart basing on S-optimality for $n > 3$. Moreover, it is shown that more than 15 observations are needed to compute higher FIM from Latin Hypercube designs with optimal Euclidean distances and S-optimality, respectively, compared to EDL design.

5.3. Computation and comparison for different parameters

The aim of this section is to emphasize the impact on the performance of the Fisher information (and its efficiency) on the four introduced designs due to changes in the parameters, i.e. by varying β.

5.3.1. Sensitivity analysis for $\alpha = 1$, $\beta = 10$, $\tilde{\sigma} = 1$

In this simulation we change the values of the parameters $\alpha, \beta, \tilde{\sigma}$ to 1, 10 and 1. Hence, the effect of an increase in β on the Fisher information can be observed. Moreover, this leads to the fact that the fraction in the correlation structure is unequal to 1, in contrast to the previous setup. Table 5 and Fig. 5 show the arithmetic mean of efficiencies of Fisher information based on 1000 experiments. Analogously, the (same) four defined designs, given the introduced change in β, are compared per (same set of) design points with respect to each other. In this setup the most efficient design varies per increased design points n. Factorial design is most efficient for n being smaller and equal to 3. Following to that, LHS computed under S-optimality condition is most efficient for n between 4 and 30 observations, whereas computations with at least 30 design points indicate LHS under optimal Euclidean distances as most efficient (note that there is a tie for $n = 30$). Computations have shown stronger increases in FIM compared to the previous parameter setup (values not reported). Accordingly, both LHS approaches perform very similarly, which can also be seen in their very similar values of efficiency for n larger than 10. Hence, Fig. 5 shows that Latin Hypercube Samples designs optimized with respect to Euclidean distances almost overlaps with LHS under S-optimality. Moreover, the difference with respect to efficiency of FIM between both LHS and EDL as well as factorial designs increases with increasing number of design points.

5.3.2. Sensitivity of the simulation for different β and n

Table 6 shows the calculations of efficiency of FIM for the introduced designs, where α respectively $\tilde{\sigma}$ are equal to 1 and β uses every integer between 1 and 10. Hence, 10 calculations for every number of observations are necessary, whereby the first column for each designs is a calculation with $\beta = 2$. In order to account for simulation errors, arithmetic mean of the efficiencies based on 1000 experiments are provided. The purpose behind this sensitivity check is to observe the impact of a misclassification of β, given the known true parameter is 2. We can conclude from this comparison that an increase in β leads to largest increases in LHS designs compared to equidistant on diagonal line design,

Table 5
Arithmetic mean of efficiency for OU-sheet of FIM for different number of design points (n), $\alpha = 1$, $\beta = 10$, $\tilde{\sigma} = 1$ with equidistant on diagonal line, factorial, LHS* (S-optimality), and LHS+ (improved LHS as optimal with respect to Euclidean distances).

n	EDL	Factorial	LHS*	LHS+
2	0.5046	1.0000	0.5043	0.5043
3	0.7528	1.0000	0.7556	0.7555
4	0.9655	0.9939	1.0000	0.9994
5	0.9084	0.7967	1.0000	0.9994
6	0.8396	0.6652	1.0000	0.9991
7	0.7710	0.5716	1.0000	0.9991
8	0.7074	0.5014	1.0000	0.9990
9	0.6507	0.4469	1.0000	0.9990
10	0.6008	0.4033	1.0000	0.9990
15	0.4290	0.2728	1.0000	0.9991
20	0.3328	0.2077	1.0000	0.9996
30	0.2316	0.1427	1.0000	1.0000
40	0.1797	0.1102	0.9996	1.0000
50	0.1482	0.0907	0.9993	1.0000
75	0.1060	0.0648	0.9989	1.0000
100	0.0849	0.0518	0.9987	1.0000

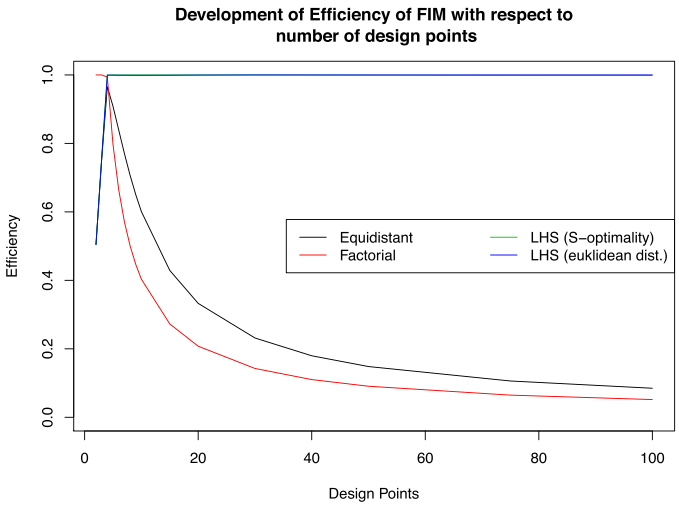

Fig. 5. Development of efficiency for OU-sheet of FIM for number of Design Points, $\alpha = 1$, $\beta = 10$, $\tilde{\sigma} = 1$.

regardless of the number of observations. Moreover, within every design we can observe higher efficiency for higher values of β. EDL design shows a better performance in terms of efficiency with respect to FIM for small numbers of design points. However, by increasing β and n one will obtain higher efficiency from Latin Hypercube designs. Due to roundings on two decimal places one obtains duplicates of highest efficiencies (equal to 1) per number of design points (Figs. 6 and 7).

5.4. Computation and comparison of variance

This section compares the variance with respect to the four known designs and the number of observations. When considering all pairs of $(s_i, t_i)\ \forall\ i = 1, \ldots, n$ one obtains a $n \times n$-covariance matrix according to (3). Hence, the sum of these elements results in an estimator of the variance. Analogously to previous computations, 1000 experiments were conducted and the arithmetic mean of the variance per design and observation number are reported in Table 7. These replicates enable to average out the simulation effects under a small scale study, i.e. small number of observations. Note that in this paper we only consider $n = 4$ for factorial design, wherefore the variance of this design remains constant. We can observe very similar variances for both LHS

Table 6
Efficiency of FIM for OU-sheet for different number of design points and different beta of equidistant on diagonal line, factorial, LHS* (S-optimality) and LHS+ (improved LHS as optimal with respect to Euclidean distances) designs.

n/β	Equidistant										Factorial										LHS with S-Optimality										LHS with optimal Euclidean distances									
	2	1	3	4	5	6	7	8	9	10	2	1	3	4	5	6	7	8	9	10	2	1	3	4	5	6	7	8	9	10	2	1	3	4	5	6	7	8	9	10
2	0.48	0.44	0.50	0.50	0.50	0.50	0.50	0.50	0.50	0.50	0.94	0.83	0.97	0.99	0.99	0.99	1.00	1.00	1.00	1.00	0.49	0.47	0.50	0.50	0.50	0.50	0.50	0.50	0.50	0.50	0.49	0.47	0.50	0.50	0.50	0.50	0.50	0.50	0.50	0.50
3	0.57	0.49	0.64	0.68	0.71	0.73	0.74	0.75	0.75	0.75	0.94	0.83	0.97	0.99	0.99	0.99	1.00	1.00	1.00	1.00	0.71	0.63	0.73	0.74	0.75	0.75	0.75	0.75	0.75	0.75	0.69	0.61	0.72	0.74	0.74	0.75	0.75	0.75	0.75	0.76
4	0.60	0.49	0.69	0.76	0.82	0.87	0.91	0.93	0.95	0.97	0.94	0.82	0.97	0.98	0.99	0.99	0.99	0.99	0.99	0.99	0.89	0.74	0.94	0.97	0.98	0.99	0.99	1.00	1.00	1.00	0.89	0.75	0.95	0.97	0.98	0.99	0.99	1.00	1.00	1.00
5	0.49	0.40	0.57	0.65	0.71	0.77	0.81	0.85	0.88	0.91	0.75	0.66	0.78	0.79	0.79	0.79	0.79	0.80	0.80	0.80	0.87	0.69	0.93	0.96	0.98	0.99	0.99	1.00	1.00	1.00	0.85	0.67	0.92	0.96	0.97	0.98	0.99	0.99	1.00	1.00
6	0.41	0.33	0.49	0.55	0.62	0.67	0.72	0.77	0.81	0.84	0.63	0.55	0.65	0.65	0.66	0.66	0.66	0.66	0.66	0.66	0.83	0.63	0.91	0.95	0.97	0.98	0.99	0.99	1.00	1.00	0.84	0.64	0.92	0.96	0.98	0.99	0.99	0.99	1.00	1.00
7	0.36	0.29	0.42	0.48	0.54	0.60	0.65	0.69	0.73	0.77	0.54	0.47	0.56	0.56	0.56	0.57	0.57	0.57	0.57	0.57	0.80	0.58	0.89	0.94	0.96	0.98	0.98	0.99	1.00	1.00	0.80	0.59	0.89	0.94	0.96	0.98	0.99	0.99	1.00	1.00
8	0.31	0.25	0.37	0.43	0.48	0.54	0.58	0.63	0.67	0.71	0.47	0.42	0.49	0.49	0.49	0.50	0.50	0.50	0.50	0.50	0.77	0.54	0.87	0.93	0.95	0.97	0.98	0.99	1.00	1.00	0.78	0.55	0.88	0.93	0.96	0.97	0.98	0.99	1.00	1.00
9	0.28	0.22	0.33	0.39	0.44	0.48	0.53	0.57	0.61	0.65	0.42	0.37	0.44	0.44	0.44	0.44	0.45	0.45	0.45	0.45	0.75	0.51	0.86	0.92	0.95	0.97	0.98	0.99	1.00	1.00	0.73	0.50	0.84	0.90	0.94	0.96	0.97	0.98	0.99	1.00
10	0.25	0.20	0.30	0.35	0.40	0.44	0.48	0.52	0.56	0.60	0.38	0.33	0.39	0.40	0.40	0.40	0.40	0.40	0.40	0.40	0.73	0.48	0.84	0.91	0.94	0.97	0.98	0.99	1.00	1.00	0.71	0.47	0.83	0.90	0.93	0.96	0.97	0.98	0.99	1.00
15	0.17	0.14	0.21	0.24	0.27	0.30	0.34	0.37	0.40	0.43	0.26	0.23	0.27	0.27	0.27	0.27	0.27	0.27	0.27	0.27	0.62	0.38	0.77	0.86	0.91	0.94	0.97	0.98	0.99	1.00	0.62	0.37	0.77	0.85	0.91	0.94	0.96	0.98	0.99	1.00
20	0.13	0.10	0.16	0.18	0.21	0.23	0.26	0.28	0.31	0.33	0.20	0.17	0.20	0.20	0.21	0.21	0.21	0.21	0.21	0.21	0.55	0.31	0.71	0.81	0.88	0.92	0.95	0.97	0.99	1.00	0.55	0.31	0.71	0.81	0.88	0.92	0.95	0.97	0.99	1.00
30	0.09	0.07	0.11	0.13	0.14	0.16	0.18	0.20	0.21	0.23	0.13	0.12	0.14	0.14	0.14	0.14	0.14	0.14	0.14	0.14	0.45	0.23	0.62	0.74	0.83	0.89	0.93	0.96	0.98	1.00	0.45	0.23	0.62	0.74	0.82	0.88	0.93	0.96	0.98	1.00
40	0.07	0.06	0.08	0.10	0.11	0.12	0.14	0.15	0.17	0.18	0.10	0.09	0.11	0.11	0.11	0.11	0.11	0.11	0.11	0.11	0.38	0.18	0.55	0.68	0.78	0.85	0.90	0.94	0.97	1.00	0.38	0.19	0.55	0.68	0.78	0.85	0.91	0.95	0.98	1.00
50	0.06	0.05	0.07	0.08	0.09	0.10	0.11	0.13	0.14	0.15	0.09	0.08	0.09	0.09	0.09	0.09	0.09	0.09	0.09	0.09	0.33	0.16	0.50	0.64	0.74	0.83	0.89	0.93	0.97	1.00	0.34	0.16	0.50	0.64	0.74	0.83	0.89	0.94	0.97	1.00
75	0.04	0.03	0.05	0.06	0.07	0.07	0.08	0.09	0.10	0.11	0.06	0.05	0.06	0.06	0.06	0.06	0.06	0.06	0.06	0.06	0.26	0.12	0.41	0.55	0.67	0.77	0.85	0.91	0.96	1.00	0.26	0.12	0.42	0.55	0.67	0.77	0.85	0.91	0.96	1.00
100	0.03	0.03	0.04	0.05	0.05	0.06	0.07	0.07	0.08	0.08	0.05	0.04	0.05	0.05	0.05	0.05	0.05	0.05	0.05	0.05	0.22	0.10	0.36	0.50	0.62	0.73	0.81	0.89	0.95	1.00	0.22	0.10	0.36	0.50	0.62	0.73	0.82	0.89	0.95	1.00

designs, decreasing from about 0.175 to 0.1419, the magnitude of the variance of the factorial design. In contrast to that, variance of equidistant design increases from 0.1317 to about 0.1413. However, it still shows smaller variance compared to the three other designs for 100 observations.

6. Application

6.1. Kriging based techniques used for estimation of mass balance

Typically Kriging interpolations are overspread in GIS softwares and one important technique may be overseen, namely a not necessary rasterization of glacier areas, where no dense measurements are taken. However, this rasterization can critically increase the unwanted variance. This is illustrated for the case of Olivares glaciers in the following examples.

In Olivares Alfa the area is represented by $N = 4731$ points for full raster and we receive a variance of $V_{4731} = 0.6001$. In the original sample of 10 stakes we receive a variance of $V_{10} = 0.6$ However, we need to point out that if a typical glaciological approach was used to compute the rest of values by kriging (based on ArcGIS), then we would neglect the variance of kriging in the full raster approach. For Olivares Beta instead we have $N = 8830$ for the full raster and computed a variance of $V_{8830} = 0.64$. In the original sample of 10 stakes we receive a variance of $V_{10} = 0.54$. Thus, we can conclude that adding full raster of points is artificial and may increase the variance of mass balance estimations. Another typically used method is geostatistical method (Thiessen poligons) (Burrough, 1986).

D and K-optimality can provide a good benchmark for applications. In this section we consider mass balance of glacier as a functional of interest. The mass balance is defined as $m_T = \frac{1}{T}\int_0^T Y(t)dt$. We will show that it is preferable to use just the observations (without the additional interpolation or extrapolation by simple kriging) in order not to increase the variance. In particular, we recall Smit's paradox Smit (1961).

6.2. The case of an OU process

Let $Y(t)$ be stationary, and $\vartheta = EY(t)$. When the process is observable on the interval $[0, T]$, the mean ϑ may be (unbiased) estimated with

$$\overline{Y}_{N+1} := \frac{1}{N}\sum_{k=0}^{N} Y(kT/N).$$

One might be inclined to expect that $\mathrm{Var}(m_T) \leq \mathrm{Var}(\overline{Y}_{N+1})$, since *"the estimator m_T utilizes the whole realization rather than a finite number of points"*. However, there are equidistant designs ξ_n for which

$$\mathrm{Var}(\overline{Y}_{N+1}) < \mathrm{Var}(m_T).$$

The following Examples 1 and 2 show that less points can decrease the variance.

Example 1. Further information on this example can be found in Example 3 of (Näther, 1985). We have $X = [-1, 1]$ and $cov(Y(x_1), Y(x_2)) = \exp(-|x_1 - x_2|)$

$$\xi_5 = \{-1, -0.5, 0, 0.5, 1\}.$$

We have $\mathrm{Var}(\overline{Y}_{N+1}) = 0.529$ and $Var(m_T) = 0.568$. To explain the paradox: in general, m_T is not the best linear unbiased estimator (BLUE) for ϑ.

The variance of $\overline{Y}$ can increase by use of additional observations:

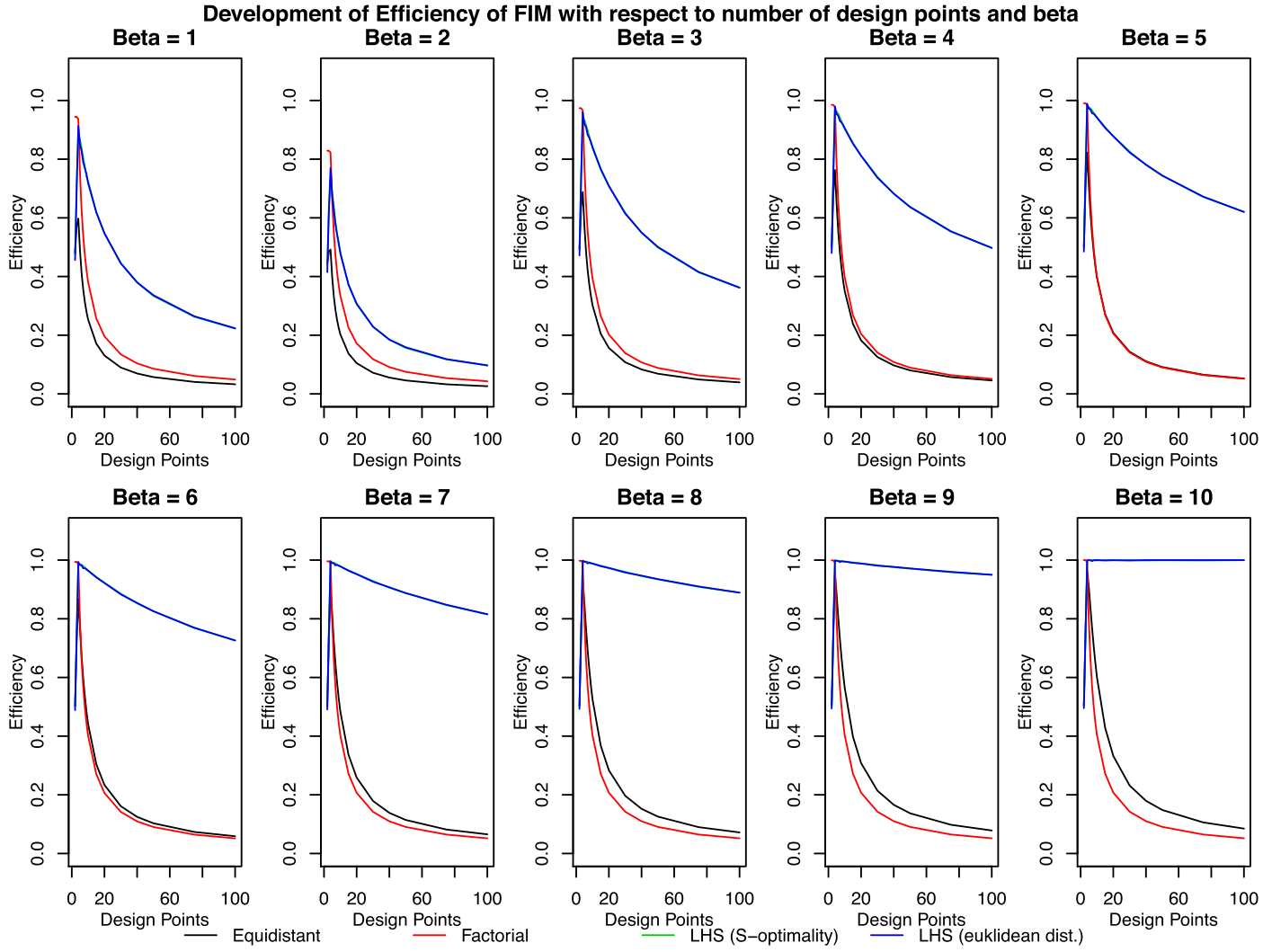

Fig. 6. Development of efficiency for OU-sheet of FIM for number of design points from 1 to 100, $\alpha = 1$, and $\beta = \{1, \ldots, 10\}$, $\tilde{\sigma} = 1$.

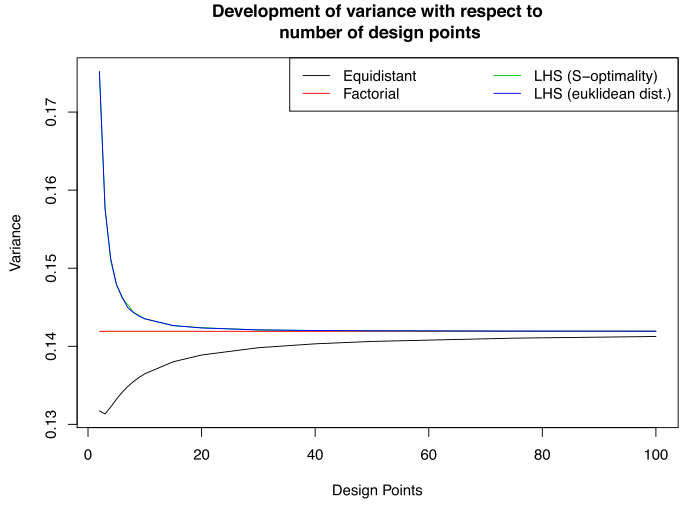

Fig. 7. Development of variance for design points from 1 to 100.

Table 7
Computation of variance according to (3) for equidistant on diagonal line, factorial, LHS* (S-optimality) and LHS+ (improved LHS as optimal with respect to Euclidean distances) designs

n	Equidistant	Factorial	LHS*	LHS+
2	0.1317	0.1419	0.1751	0.1752
3	0.1313	0.1419	0.1577	0.1576
4	0.1322	0.1419	0.1509	0.1512
5	0.1332	0.1419	0.1479	0.1479
6	0.1341	0.1419	0.1462	0.1463
7	0.1348	0.1419	0.1453	0.1449
8	0.1355	0.1419	0.1443	0.1443
9	0.1360	0.1419	0.1439	0.1439
10	0.1365	0.1419	0.1435	0.1435
15	0.1380	0.1419	0.1426	0.1427
20	0.1389	0.1419	0.1424	0.1423
30	0.1398	0.1419	0.1421	0.1421
40	0.1403	0.1419	0.1420	0.1420
50	0.1406	0.1419	0.1420	0.1420
75	0.1410	0.1419	0.1419	0.1419
100	0.1413	0.1419	0.1419	0.1419

Example 2. This example considers Example 4 of (Näther, 1985). Thereby, we have $X=[-1, 1]$, $cov(Y(x_1), Y(x_2))=\exp(-|x_1-x_2|)$ and $\xi_5=\{-1, -0.5, 0, 0.5, 1\}$, ξ_9 are equidistant designs.We obtain $\mathrm{Var}(\overline{Y}(\xi_5))=0.529$ and $\mathrm{Var}(\overline{Y}(\xi_9))=0.542$. However, the BLUE-variance is 0.5.

Thus, we can conclude averaging over the points obtained from OU process may increase variance of the arithmetic mean.

6.3. What is happening for case of OU-sheet?

In order to detect the effect in the case of OU-sheet we start by providing Example 3.

Example 3. Let us check how big is the chance to get a decrease of variance for OU sheet defined over $[0,1]^2$, when we have $\alpha=1$, $\beta=0.5$ and we compare the variance for mean evaluated for (1) two point design $D_2:=\{(0, 0), (t, s)\}$ (2) three point design, where mid point $(s/2, t/2)$ is added to design D_2.We received that $V(\overline{X}_2)=\frac{2+2\exp(-x)}{4}$ and $V(\overline{X}_3)=\frac{3+4\exp(-x/2)+2\exp(-x)}{9}$, where $x=s+t/2$.We have a boundary line $x=-2\ln\frac{3}{5}$ on which $V(\overline{X}_3)-V(\overline{X}_2)$ is changing the sign. This means that, based on geometric probability, we have 88% of probability to increase variance by adding a 3rd point.

Therefore, more care should be taken in designing for mass balance measurements on glaciers. The next subsection illustrates this fact on simulated data. The parameter sensitivity can be observed in Tables 8 and 9 for the process defined in (1), while for the sheet defined in (3) the results can be found in Table 10.

6.4. Linear relationship between mass balance and altitude

The relationship between altitude and mass balance has been addressed in several works, such as Rasmussen and Andreassen (2005) where linear regularity was found in 10 Norwegian glaciers and a measurement at one altitude was developed, while in Kuhn (1984) a glacier classification criteria was developed by exploiting the mass balance profile on altitude. This latter work followed the one in Lliboutry (1974), where the mass balance at a certain location on the glacier (or altitude) is decomposed into the sum of its spatial and temporal contributions. In Cogley (1999) the correlation between time series of stakes' measurements was discussed, concluding that stakes closer to each other were highly correlated and this correlation decreased with higher altitude differences. Therefore, making more measurements in the vicinity of a stake will not necessarily add new information. The optimal number of stakes is discussed in Fountain and Vecchia (1999) where two equations, a quadratic regression, and a piecewise

Table 8
Computation of the variance of an OU process with covariance structure defined in (1), and using $r=\{0.1, 5, 10\}$. Equispaced design on [0, 1] of five points was considered.

r	0.1	5	10
ξ_5	0.924	0.228	0.202

Table 9
Computation of the variance of an OU process with covariance structure defined in (1), using $r=\{0.1, 5, 10\}$ and $\sigma=\{0.1, 10\}$. Equispaced design on [0, 1] of five points was considered.

σ/r	0.1	5	10
0.1	0.207	0.200	0.200
10	72.676	2.997	0.417

Table 10
Computation of the variance of an OU sheet with covariance structure defined in (3), a regular grid on $[0, 1]\times[0, 1]$ of $\{5^2, 9^2, 17^2\}$ points was considered.

α/β	0.1	1	10
5^2 **points**			
0.1	0.8551924	0.4891167	0.18695728
1	0.4891167	0.2797442	0.10692790
10	0.1869573	0.1069279	0.04087153
9^2 **points**			
0.1	0.8647388	0.50394437	0.11956635
1	0.5039444	0.29368398	0.06967976
10	0.1195663	0.06967976	0.01653229
17^2 **points**			
0.1	0.87050431	0.51586037	0.09532551
1	0.51586037	0.30569857	0.05648984
10	0.09532551	0.05648984	0.01043872

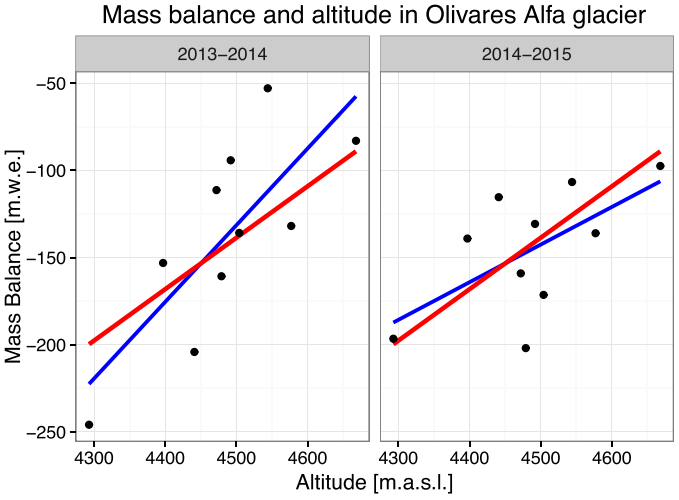

Fig. 8. Mass balance and altitude of the stakes located in Olivares Alfa glacier, for periods 2013–2014 and 2014–2015. Both linear regression (in blue), and generalized regression (in red) are plotted. (For interpretation of the references to color in this figure legend, the reader is referred to the web version of the article.)

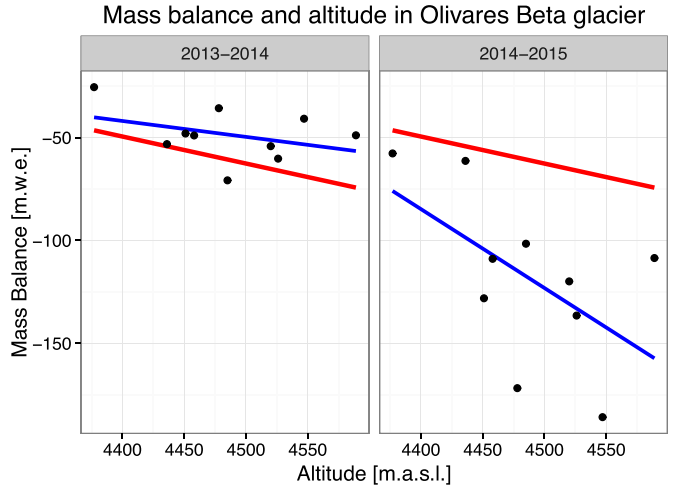

Fig. 9. Mass balance and altitude of the stakes located in Olivares Beta glacier, for periods 2013–2014 and 2014–2015. Both linear regression (in blue), and generalized regression (in red) are plotted. (For interpretation of the references to color in this figure legend, the reader is referred to the web version of the article.)

Table 11
Coefficient of determination for regressions of mass balance and altitude.

	Olivares Alfa		Olivares Beta	
	2013–2014	2014–2015	2013–2014	2014–2015
Linear	0.94	0.96	0.93	0.91
Generalized	0.92	0.95	0.86	0.64

weighted linear spline, involving mass balance and altitude are studied. This work concludes that the number of stakes appears to be scale invariant and that five to ten stakes are enough.

In Figs. 8 and 9 the profile of mass balance and altitude for two seasons can be seen. Two regressions are fitted, a linear one (in blue) and a generalized one (in red) which includes the correlation, parameters for the latter are computed as:

$$\hat{\beta} = \left\{ \text{argmin}_{\beta} (X_i\beta - Y)^T C^{-1} (X_i\beta - Y) \right\} = (X_i^T C^{-1} X_i)^{-1} X_i^T C^{-1} Y,$$

where Y is a vector of mass balance measurements, X_i is the design matrix of glacier $i = 1, 2$ (Alfa or Beta). This matrix includes components for the intercept and slope (linear relationship with altitude) of the regression, while C is a matrix defined as:

$$C = \sum_{i=1}^{2} (X_i - \overline{X}_i)(X_i - \overline{X}_i)^T + I,$$

here $\overline{X}_i$ denotes the mean of the mass balance in glacier i, and the regularization matrix I with entries equals to one in the diagonal and zero otherwise. This regularization allows to avoid the singularity of matrix C. The coefficient of determination (R^2) of both regressions on the two glaciers can be seen in Table 11.

This example shows that for some glaciers linear regression is oversimplifying the dependence on altitude. Thus in general one should test several higher order models, before automatic usage of parsimonious linear regression.

6.5. Coefficient of variation and the optimal number of stakes

The logistics for a mass balance program of a glacier can be very difficult and costly. One big goal of these programs is to obtain the most reliable information while minimizing costs. This is why it is of interest to minimize the number of stakes used in the mass balance programs (Fountain and Vecchia, 1999). In order to study several stakes' designs, the coefficient of variation of all possible configurations after the removal of one to five stakes is computed. First, stakes coordinates are transformed from latitude and longitude units to UTM 19S, and then normalized to the unit square $[0, 1] \times [0, 1]$, as it can be seen in Fig. 10.

All possible designs after the removal from one to five stakes are listed. Their coefficients of variation are computed when the parameters of the OU sheet covariance matrix are $\alpha = 0.59$ and $\beta = 2.3$. These parameters are chosen by marginal correlations of lag one. The results of this methodology can be seen in the two boxplots of Fig. 11.

The design after the removal of 5 stakes, which minimized the coefficient of variation for each glacier, can be seen in Fig. 12. A

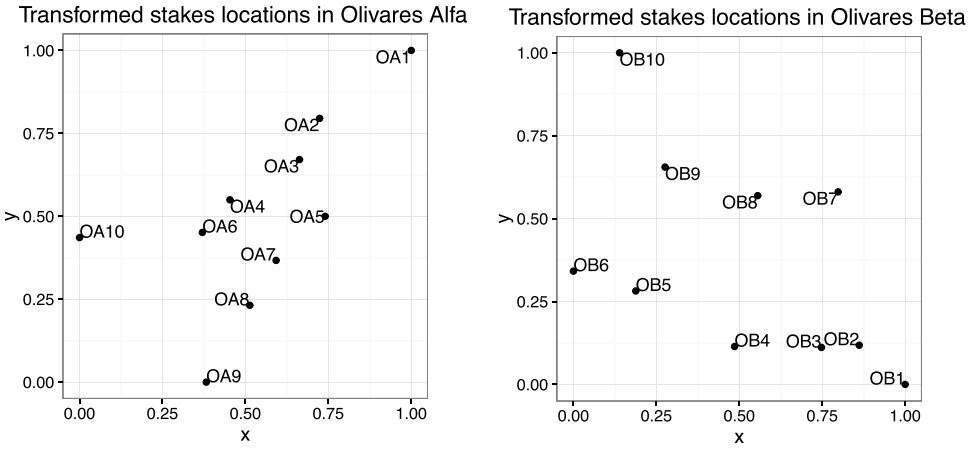

Fig. 10. Transformed stakes' locations to the domain $[0, 1] \times [0, 1]$ of glaciers Olivares Alfa and Olivares Beta.

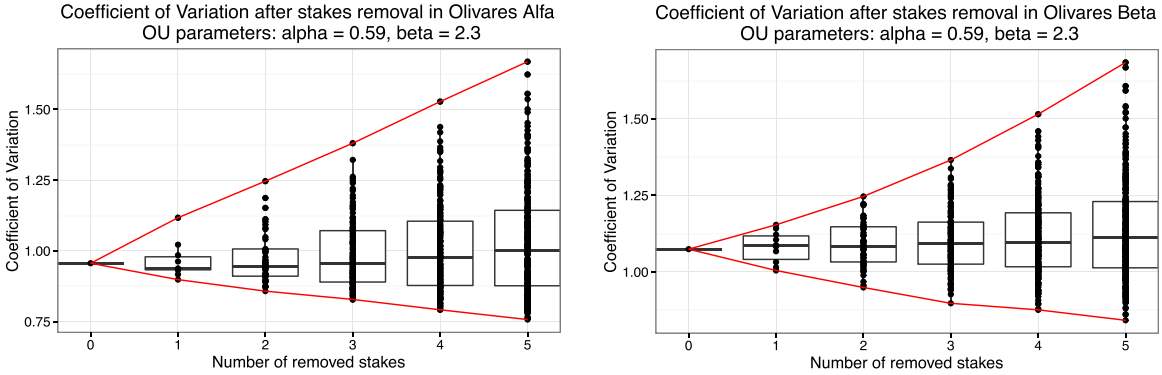

Fig. 11. Boxplot of the coefficient of variation computed over all possible designs after removing stakes in the Olivares Alfa and Olivares Beta glaciers. The parameters used for the OU sheet covariance matrix are $\alpha = 0.59$, and $\beta = 2.3$.

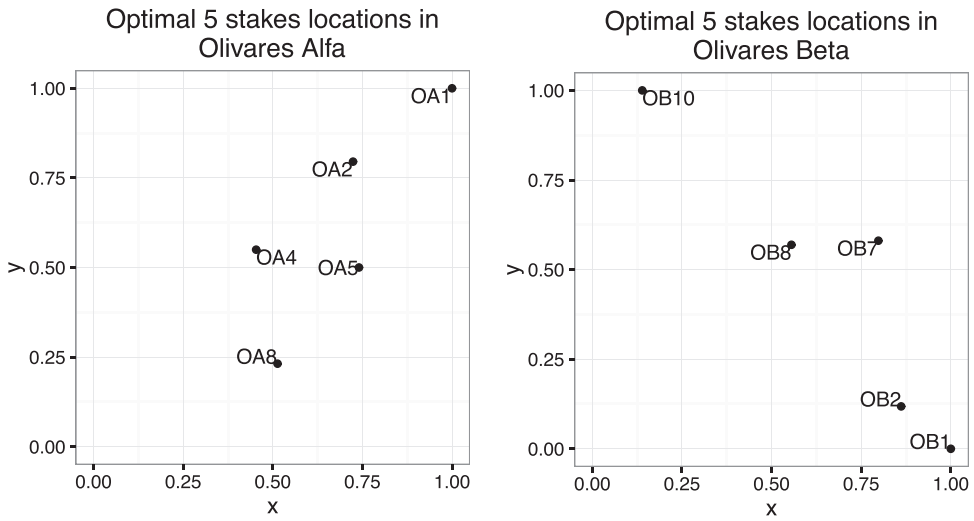

Fig. 12. Optimal locations, in the sense of minimizing the design coefficient of variation, of 5 stakes over Olivares Alfa and Olivares Beta glaciers, using an OU sheet covariance structure with $\alpha = 0.59$ and $\beta = 2.3$.

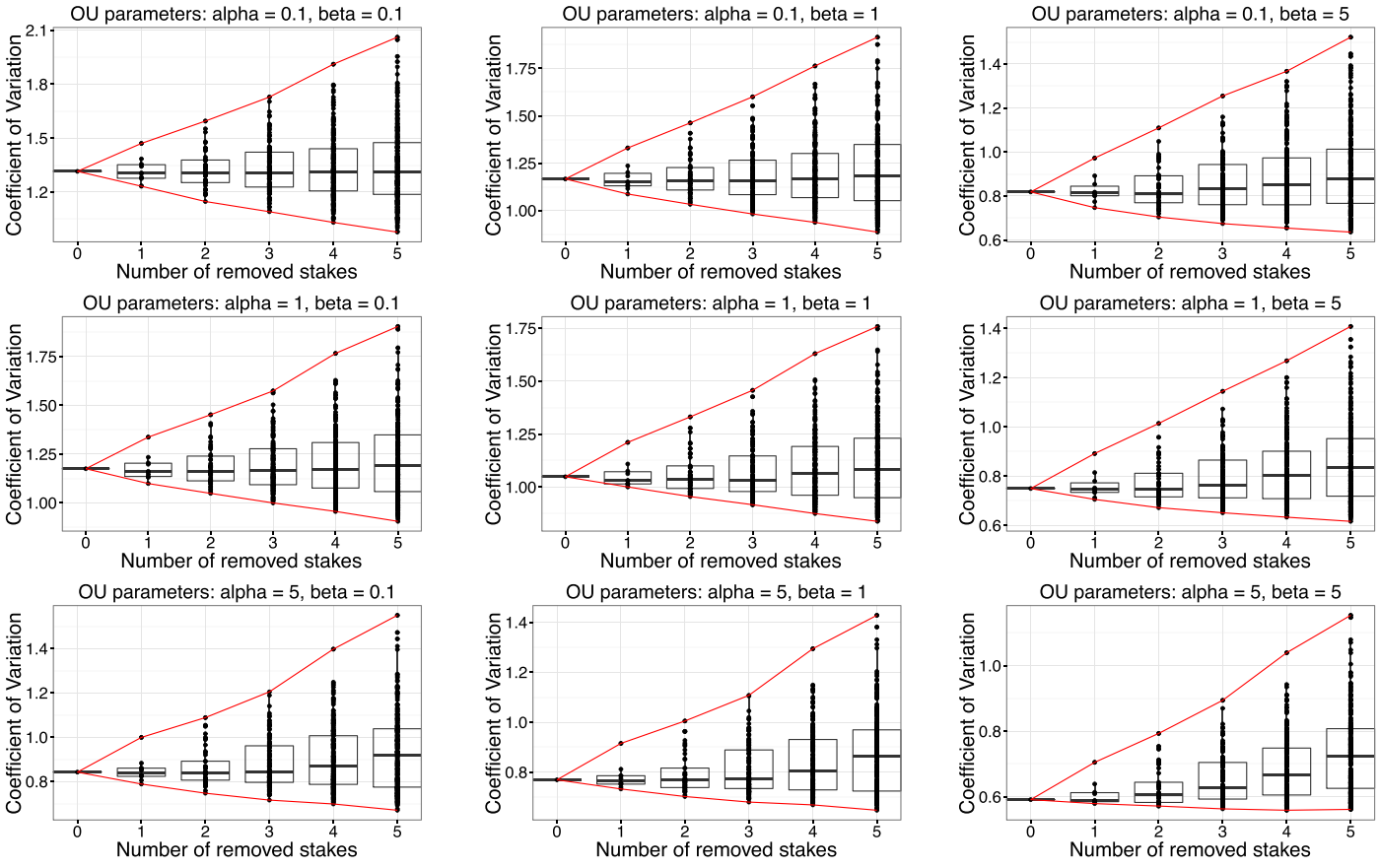

Fig. 13. Boxplot of the coefficient of variation computed over all possible designs after removing stakes in the Olivares Alfa glacier. The parameters used for the OU sheet covariance matrix are α, $\beta = \{0.1, 1, 5\}$.

sensitivity analysis is also computed by allowing parameters α and β to take values in the set $\{0.1, 1, 5\}$, as we can see in Figs. 13 and 14. As the parameters grow bigger (implying more independent data), the removal of stakes always increases the coefficient of variation. However, in the presence of dependent data (smaller values of α and β) it is possible to decrease the coefficient of variation if a good design is chosen. This clever selection allows us to decrease the dispersion in our measurement and to obtain more reliable data.

7. Dynamical system for measurements

7.1. Singularities and increase of Variance

Here we illustrate an interesting special case of the Ornstein–Uhlenbeck process, generated by

$$dx_t = -r\,x_t\,dt + \sigma\,dW_t, \quad r > 0,$$

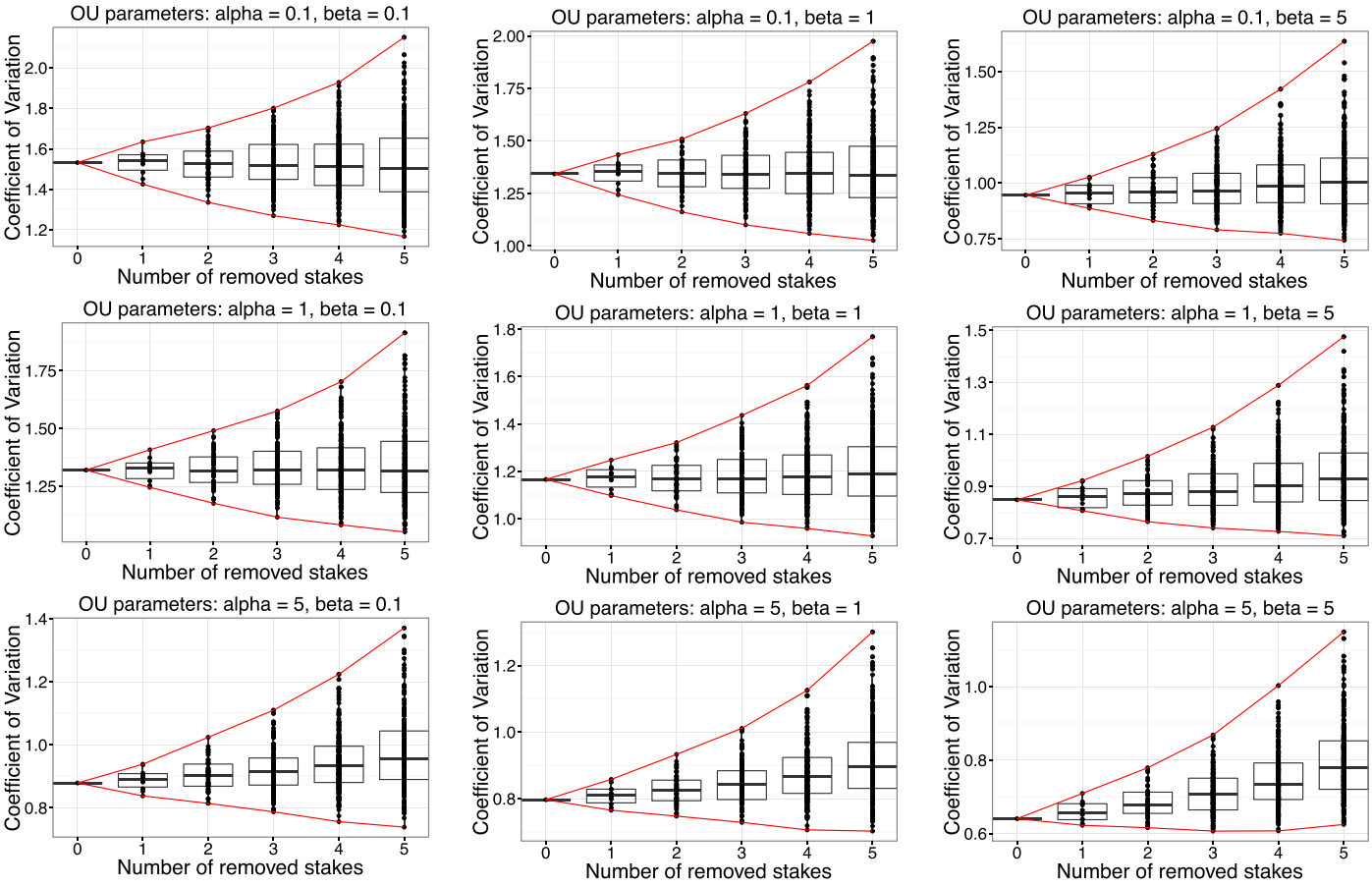

Fig. 14. Boxplot of the coefficient of variation computed over all possible designs after removing stakes in the Olivares Beta glacier. The parameters used for the OU sheet covariance matrix are α, $\beta = \{0.1, 1, 5\}$.

when r approaches zero with σ becomes infinite in such a way, that $r\sigma^2$ approaches a fixed constant (see Rybicki, 1994). Usually it is accomplished by letting $\sigma^2 = \frac{D}{2r}$, where D is a constant, called the diffusivity. This limiting case is often called the Gaussian random walk process. The correlation function $\sigma^2 e^{-rd}$ of the random walk may not be defined in such a setup, since we have singularity

$$\sigma \to +\infty \quad as \quad r \to 0^+. \tag{6}$$

However, the variogram defined as

$$\psi(\tau) = E([x_t - x_{t+\tau}]^2) = 2\sigma^2(1 - e^{-r|\tau|}) = \frac{D}{r}(1 - e^{-r|\tau|})$$

has meaning in the limit, namely $\psi(\tau) = D|\tau|$. In Stehlík and Kiseľák (2016) it was shown that also the limit $r \to 0^+$ together with $\sigma = \sqrt{2r}$ gives an interesting interpretation for the blow up of the limit of the regular solutions of the sequence of Dirichlet problems for the Poisson equation.

The behavior of variance of arithmetic mean $\mathrm{Var}(\frac{1}{m}\sum_{i=1}^{m} X_i)$, under singularity (6) can have several modalities. To illustrate this, we consider the general variance decomposition of the form

$$Var[\overline{X}] = \frac{1}{m^2}\sum_{i=1}^{m} Var[X_i] + \frac{2}{m^2}\sum_{1 \le i < j \le m} \mathbb{C}ov[X_i, X_j].$$

Let us have a look on four following scenarios. Here we assume that observations are measured at equidistant points.

- Assume that $\hat{\sigma}$ does not depend on the number of observations m but $\hat{r}$ does such that $rd \approx \ln m$ for every two consecutive

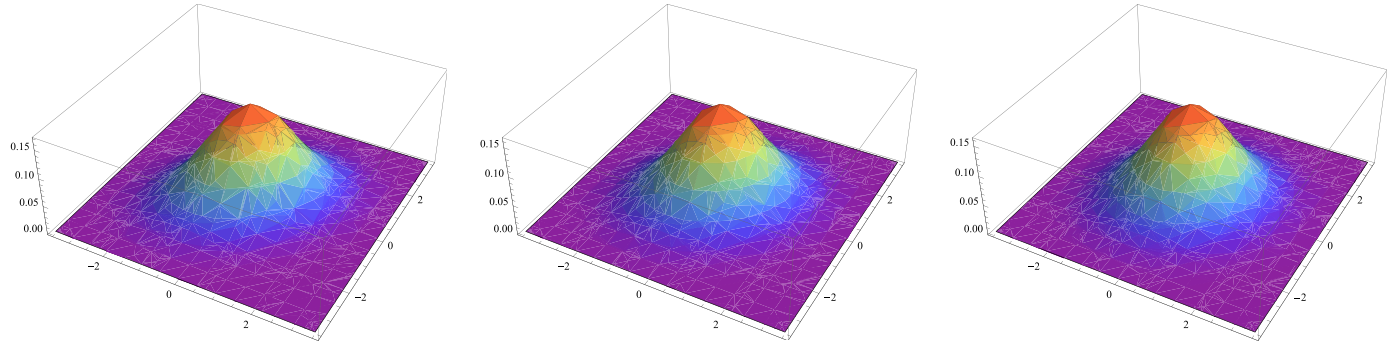

(a) $|s_1 - t_1| = 0.1$ (b) $|s_1 - t_1| = 0.5$ (c) $|s_1 - t_1| = 1$

Fig. 15. Densities h depending on distance $|s_1 - t_1| \in [0, 1]$ for fixed $\alpha = \sigma = \beta = 1$ and distance $|s_2 - t_2|$ equal 1.

observations. Then $\mathbb{C}\mathrm{ov}[X_i,X_j] = \mathrm{e}^{-(j-i)\ln m} = \frac{1}{m^{j-i}}$, where $j-i \geq 1$. Then for $m \to \infty$ rd goes to infinity and

$$Var[\overline{X}] \approx \frac{\sigma^2}{m} + \frac{m-1}{m^2} \to 0.$$

- Assume now that $\hat{\sigma}$ does not depend on the number of observations m but $\hat{r}$ does such that $(j-i)rd \ll 1$, $j-i \geq 1$. Then $\mathbb{C}\mathrm{ov}[X_i,X_j] \approx 1$ yields

$$Var[\overline{X}] \approx \frac{\sigma^2}{m} + \frac{m-1}{m} \to 1$$
for $m \to \infty$.

- Let $\hat{\sigma}$ depend on m, such that it goes to infinity for large m more quickly than $\sqrt{m}$ and rd does not. Then we have

$$Var[\overline{X}] \approx \frac{\sigma^2(m)}{m} + \frac{m-1}{m}K \to \infty$$
for $m \to \infty$, where $K > 0$ is a constant.

- Assume finally that $\hat{\sigma} = \hat{\sigma}(m) \to \sqrt{C} > 0$ (in practical situation C is large enough for specific finite value of m, e.g. C is not such $mC \ll 1$) for $m \to \infty$ and $\hat{r}$ such that $rd \approx \ln\ln(m+1) - \varepsilon \ln m$ for $\varepsilon > 0$ such that $\ln(m+1) > m^{\varepsilon}$. Thus, we can conclude that

$$Var[\overline{X}] \approx \frac{C}{m} + \frac{m-1}{m} C\, \mathrm{e}^{\varepsilon \ln m - \ln\ln(m+1)} = \frac{C}{m} + C\frac{(m-1)}{m}\frac{m^{\varepsilon}}{\ln(m+1)}$$

for $m \to \infty$. Hence, we can see that under certain developments of dynamical system for measurements, we can get very high variance for the increasing number of stakes.

7.2. Analytical description of dynamical systems and blow-ups

Consider now the stochastic process

$$Y(\mathbf{t}) = \mu(\mathbf{t}) + \varepsilon(\mathbf{t}), \tag{7}$$

where $\varepsilon(\mathbf{t})$ is a zero mean Gaussian process with stationary exponential covariance function $C(\varepsilon(\mathbf{s}),\varepsilon(\mathbf{t})) = p(\sigma,\mathbf{r})\,\mathrm{e}^{-\langle \mathbf{r}, |\mathbf{s}-\mathbf{t}| \rangle}$, $\mathbf{s},\mathbf{t} \in \mathbb{R}^n$, $\mathbf{r} \in \mathbb{R}^n_+$, $\sigma > 0$, $|\mathbf{s}-\mathbf{t}| := |s_1 - t_1|, \ldots, |s_n - t_n|$ and continuous function p.

The relationship between the Gaussian distribution and the heat equation (also called the diffusion equation) is evident. From now we fix all time variables except for one. Moreover, for the density h of Y we can conclude the following. Let $\mathbf{\Sigma}_{k,l} := C(\varepsilon(\mathbf{t^k}), \varepsilon(\mathbf{t^l}))$, $k, l = 1, \ldots, m$ and $\frac{\partial}{\partial t_i}\mathbf{\Sigma} =: \mathbf{D}^i$, $i = 1, \ldots, n$ which exists a.e., then

$$\begin{aligned} \frac{\partial}{\partial t_i} h &= \frac{1}{2}\sum_{k,l=1}^{m} \mathbf{D}^i_{k,l} \frac{\partial}{\partial y_k \partial y_l} h - \sum_{k}^{m} \frac{\partial}{\partial t_i}\mu \frac{\partial}{\partial y_k} h \\ \lim_{t_i \to 0^+} h &= \delta, \text{ for all others times being fixed zero} \end{aligned} \tag{8}$$

in which the limit is as usual understood in the weak sense. This follows directly from the form of derivatives. Clearly, if the normal density function h (with covariance matrix $\mathbf{\Sigma}$) satisfies problem (8), then

$$|\det\mathbf{\Sigma}|^{-1}\frac{\partial}{\partial t_i}\det\mathbf{\Sigma} = \mathrm{tr}(\mathbf{D}^i\mathbf{\Sigma}^{-1}) \text{ and } \frac{\partial}{\partial t_i}\mathbf{\Sigma}^{-1} = -\mathbf{\Sigma}^{-1}\mathbf{D}^i\mathbf{\Sigma}^{-1}$$

must hold. Nevertheless, $\frac{\partial}{\partial t_i}\left(\mathbf{\Sigma}\mathbf{\Sigma}^{-1}\right) = \mathbf{0}$ implies $\frac{\partial}{\partial t_i}\mathbf{\Sigma}^{-1} = -\mathbf{\Sigma}^{-1}\left(\frac{\partial}{\partial t_i}\mathbf{\Sigma}\right)\mathbf{\Sigma}^{-1}$. Therefore, the second condition is fulfilled if $\frac{\partial}{\partial t_i}\mathbf{\Sigma} = \mathbf{D}^i$ holds. On the other hand Jacobi's formula gives us directly that also the first condition holds under this assumption. But this means that our process is closely related to the diffusion problem (8). We will now discuss the relation to linear dynamical system. Definition 1 can be understood as a generalization of the matrix exponential function. This allows us to study this problem as a dynamical system (Figs. 15–17).

Definition 1. A family $T(t)$ of bounded linear operators on X to X is said to be a C_0-*semigroup* (or linear dynamical system) on X if $T(0)h = h$ and $T(t+s)h = T(t)T(s)h$ for all $s,t \in \mathbb{R}^+$ and if $T(t)h$ is continuous in (t, h) on $\mathbb{R}^+ \times X$.

The semigroup condition is nothing else than an expression of the Markov property. Problem (8) can be understood as the abstract IVP

$$\dot{h}(t_i) = A\,h(t_i),\ h(0) = h_0 \in D(A) \text{ for } t_i \in \mathbb{R}^+,$$

where $A : D(A) \to X$ is a linear operator defined by rhs of (8) on dense domain $D(A)$ in X. The trajectories $h(t_i, h_0) = T(t_i)h_0$, for $h_0 \in X$ but $h_0 \notin D(A)$, are called general solution. Here, by multiplication $T(t_i)h$ we mean a convolution. Then for f bounded and measurable

$$T(t_i)f(\mathbf{x}) = \int_{\mathbb{R}^n} f(\mathbf{y})\,h(t_i; \mathbf{x}-\mathbf{y})d\mathbf{y}.$$

Notice that the infinitesimal generator A of a strongly continuous semigroup T is defined by

$$Af = \lim_{t_i \downarrow 0}\frac{(T(t_i) - \mathrm{id})f}{t_i} = \lim_{t_i \downarrow 0}\frac{E^{\mathbf{y}}[f(Y(t_i))] - f(\mathbf{y})}{t_i}$$

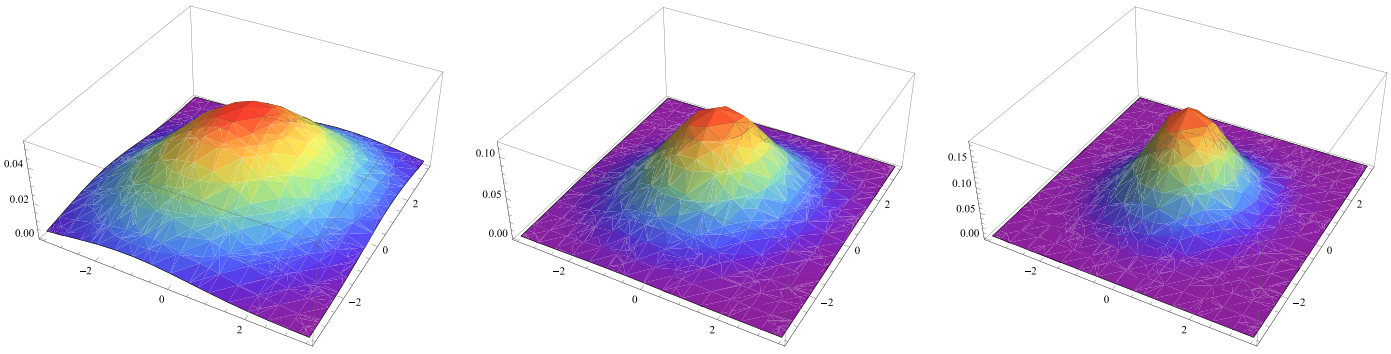

(a) $\beta = 0.1$ (b) $\beta = 0.5$ (c) $\beta = 1.3$

Fig. 16. Densities h depending on parameter $\beta \in [0, 1.3]$ for fixed $\alpha = \sigma = 1$ and distances equal 1.

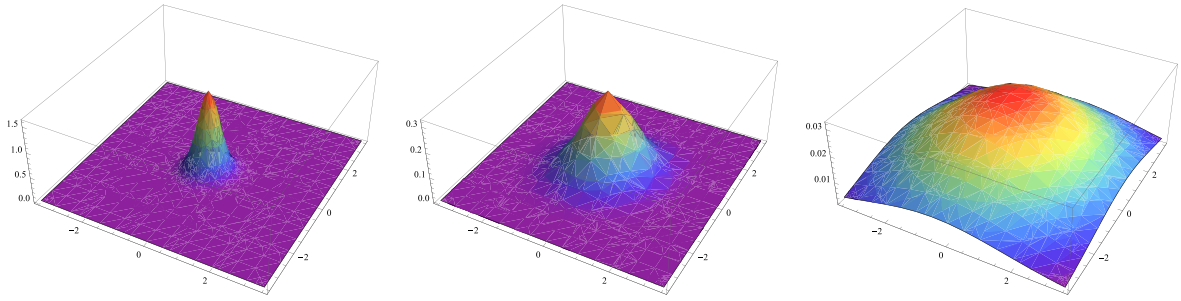

(a) $\sigma = 0.1$ (b) $\sigma = 0.5$ (c) $\sigma = 5$

Fig. 17. Densities h depending on parameter $\sigma > 0$ for fixed $\alpha = \beta = 1$ and distances equal 1.

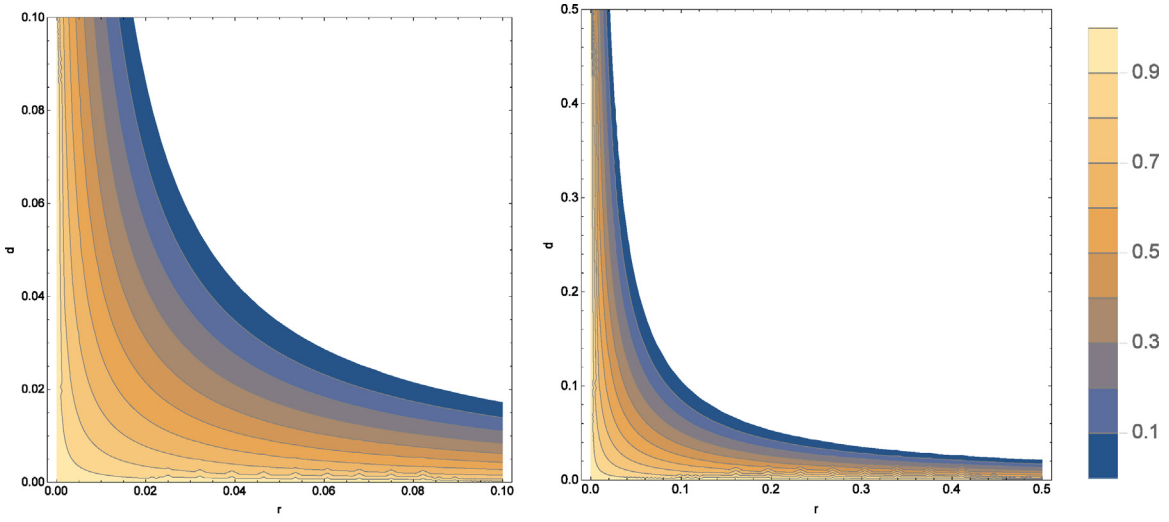

(a) $C = 1$ (b) $C = 0.1$

Fig. 18. Contours of probability $\mathcal{P}$ for process (1) for fixed $\mathbf{r}$, two values C.

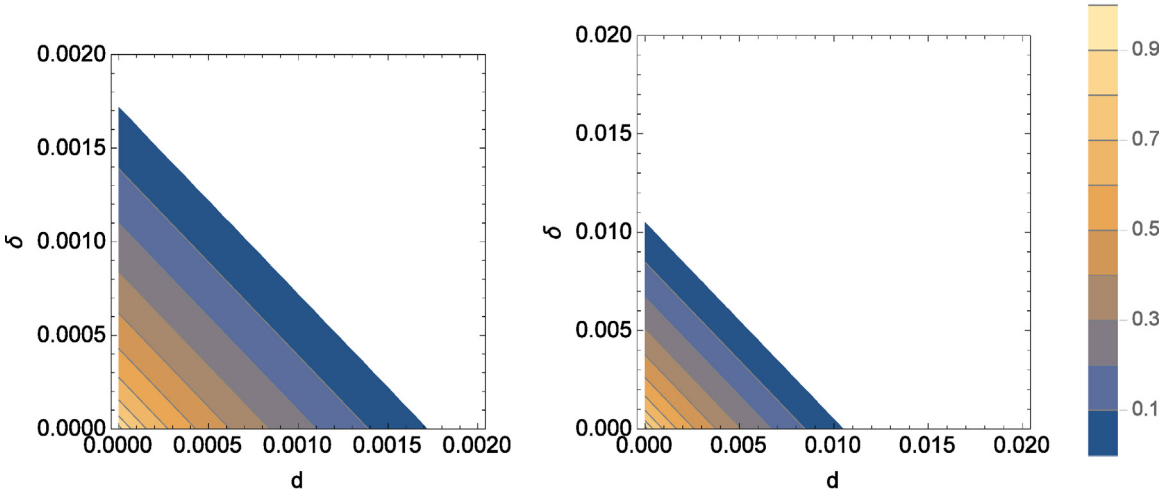

(a) $C = 1$ (b) $C = 0.1$

Fig. 19. Contours of probability $\mathcal{P}$ for process (2) with $\alpha = \beta = 1$ for two values C.

whenever the limit exists and for the family of processes $Y(\mathbf{t})$ we can define the associated Markov semigroup by the conditional formula

$$T(t_i)f(\mathbf{y}) = E[f(Y(t_i))|Y(0) = y]$$

We now show that the semigroup can generate a stochastically unbounded system in some sense. Theorem 1 says that it strictly depends on the diffusion matrix (which yields covariance structure).

Theorem 1. *If*

$$\lim_{\substack{\mathbf{r} \to \mathbf{0} \\ \mathbf{r} \in \mathbb{R}^n_+}} p(\sigma,\mathbf{r}) \sqrt{1 - e^{-2\langle \mathbf{r}, |\mathbf{s}-\mathbf{t}| \rangle}} = 0,$$

then the systems $\{\ln h(Y(\mathbf{t});\mathbf{r})\}_{\mathbf{r}>\mathbf{0}}$ *and* $\{h(Y(\mathbf{t});\mathbf{r})\}_{\mathbf{r}>\mathbf{0}}$ *are stochastically unbounded.*

Proof. Without loss of generality we consider $m=2$. Set $\bar{\mathbf{t}} = (\mathbf{t}^1,\mathbf{t}^2) = (\mathbf{t},\mathbf{s})$ and $|\mathbf{s}-\mathbf{t}| = \mathbf{d}$. Then $\mathbf{Y}(\bar{\mathbf{t}}) \sim \mathcal{N}([\mu(\mathbf{t}),\mu(\mathbf{s})]^T,\boldsymbol{\Sigma})$, where $\boldsymbol{\Sigma} = p(\sigma,\mathbf{r})\begin{pmatrix} 1 & q \\ q & 1 \end{pmatrix}$, $q = \mathrm{e}^{-\langle \mathbf{r},\mathbf{d}\rangle}$. It is easy to check that $\det\boldsymbol{\Sigma} \to 0$, for $\mathbf{r} \to \mathbf{0}$ and from continuity of the map $\mathbf{r} \to \boldsymbol{\Sigma}(\mathbf{r})$ we also have $\det\boldsymbol{\Sigma}(\mathbf{0}) = 0$. Now let $C>0$ be arbitrary constant. Nevertheless $\boldsymbol{\Sigma}^{-1}$ and $\mathrm{tr}\boldsymbol{\Sigma}^{-1}$ does not change its sign. This means that under one additional (see inequality below) $\boldsymbol{\Sigma}$ generates an ellipse $\mathcal{Y} = \{\mathbf{y} : \mathbf{y}^T\boldsymbol{\Sigma}^{-1}\mathbf{y} < -2\ln(2\pi\mathrm{e}^C(\det\boldsymbol{\Sigma})^{1/2})\}$ (here we have used the fact that the problem is invariant under affine transformation). Since

$$\mathcal{P} := \mathbb{P}(\ln h(Y(\bar{\mathbf{t}});\mathbf{r}) > C) = \int_{\mathcal{Y}} d\nu(\mathbf{y}),$$

we have for

$$\mathbf{r} > \mathbf{0} : \ \langle \mathbf{r},\mathbf{d}\rangle < -\frac{1}{2}\ln\left(1 - \frac{\mathrm{e}^{-2C}}{4\pi^2}\right),$$

the formula (Gaussian measure of $\mathcal{Y}$) $\mathcal{P} = 1 - 2\pi\mathrm{e}^C p(\sigma,\mathbf{r})\sqrt{1-q^2}$. So finally $\lim_{\substack{\mathbf{r}\to\mathbf{0} \\ \mathbf{r}\in\mathbb{R}^n_+}} \mathcal{P} = 1$.

This theorem can be applied for the process (1), where $n=1$, $\mu(t) = \alpha_1 + \alpha_2 t$, $\mathbf{r} = r$, $p(\sigma,\mathbf{r}) = 1$ and $q = \mathrm{e}^{-r|s-t|}$. Notice that it does not hold for the process (2), where $n=2$, $\mu(t) = \theta$, $\mathbf{r} = (\alpha,\beta)$, $p(\sigma,\mathbf{r}) = \frac{\tilde{\sigma}}{2\sqrt{\alpha\beta}}$ and $q = \mathrm{e}^{-\alpha|t_1-s_1|-\beta|t_2-s_2|}$, since $\lim_{\substack{\mathbf{r}\to\mathbf{0} \\ \mathbf{r}\in\mathbb{R}^n_+}} \mathcal{P}$ is not zero. In fact it does not exist (Figs. 18 and 19).

The authors in Stehlík and Kiseľák (2016) showed that also a process given by the two dimensional system of linear stochastic differential equations

$$d\mathbf{X}_t = (\mathbf{A}(t)\mathbf{X}_t + \mathbf{a}(t))\,dt + \boldsymbol{\sigma}(t)\,d\mathbf{W}_t,\ 0 \le t < \infty, \quad \mathbf{X}_0 = \boldsymbol{\xi}. \tag{9}$$

$\mathbf{a}(t) \equiv 0$ and constant coefficients $\mathbf{A} = \mathrm{diag}(-r_1, -r_2)$ and $\boldsymbol{\sigma} = \mathrm{diag}(\sqrt{2r_1},\sqrt{2r_2})$, $\mathbf{Q} = \mathbf{I}$ and $\boldsymbol{\xi} \sim \mathcal{N}(\mathbf{0},\mathbf{I})$, is stochastically unbounded.

Remark 1. They also showed that blow-up occurs for two dimensional (dependent) process given by system (9), whereas $\mathbf{a}(t) \equiv 0$ and $\boldsymbol{A}(t) = \begin{pmatrix} -r_1 & 0 \\ -r_2 & 0 \end{pmatrix}$, $\boldsymbol{\sigma} = \begin{pmatrix} \sigma & 0 \\ 0 & 0 \end{pmatrix}$ with $\mathbf{Q} = \mathbf{I}$ and $\boldsymbol{\xi} \sim \mathcal{N}(\mathbf{0},\mathbf{I})$, whereas the process $\mathbf{X}_t = (X^1_t, -r_2\int_0^t X^1_s\,ds)$, is the Ornstein–Uhlenbeck process and its time integral, which is also Gaussian.

8. Conclusions

The moderate number of stakes for small glaciers ($<10\,\mathrm{km}^2$) has been an empirically well observed fact. However, there was a lack of theoretical justifications. This paper aims to overcome this gap. We introduce a 2nd order spatial field model for mass balance measurements and evaluate its aggregated value, namely empirical mass balance. We derive a dynamical system and show that under its generic singularity, variance of mass balance estimator can grow with the number of stakes. This phenomenon relates both to blow-ups and severe interrelations between parameters and design points for stakes.

We also studied good design strategies for stakes allocations. We illustrated that monotonic design should be taken as an interesting benchmark design for cases when researchers expect non-reversibility of time (process cannot step back in time). In fact we have seen that efficiencies for monotonic designs are comparable (if not better in certain setups) to the efficiency of space-filling designs. More discussion and statistical derivation can be found in Baran and Stehlík (2015). We also compared several designs, namely equidistant, factorial, LHS* (S-optimality) and LHS+ (improved LHS as optimal with respect to Euclidean distances). These kind of designs can be of help for mass balance computations in glaciology, where simple application of full raster design can lead to increased variance, which is undesirable. This was also illustrated on real data example for Chilean glaciers *Olivares Alfa* and *Beta* and its stakes locations, where if we assume certain covariance structure, the removal of stakes can lead to a variance increase or decrease, showing us the importance of the underlying design.

Acknowledgments

Milan Stehlí k and S. Torres Leiva acknowledge FONDECYT Regular 2015, No1151441: “Statistical and mathematical modelling as a knowledge bridge between Society and Ecology Sustainability”. We also acknowledge the support of the ANR project DESIRE FWF I 833-N18, project LIT-2016-1-SEE-023 and WTZ Project SK09/2016.

References

Baran, S., Sikolya, K., Stehlík, M., 2013. On the optimal designs for prediction of Ornstein–Uhlenbeck sheets. Stat. Prob. Lett. 83 (6), 1580–1587.
Baran, S., Stehlík, M., 2015. Optimal designs for parameters of shifted Ornstein–Uhlenbeck sheets measured on monotonic sets. Stat. Prob. Lett. 99, 114–124.
Boukouvalas, A., Cornford, D., Stehlík, M., 2014. Optimal design for correlated processes with input-dependent noise. Comput. Stat. Data Anal. 71, 1088–1102.
Burrough, P.A., 1986. Principles of geographical information systems for land resources assessment. Geocarto Int. 1 (3), 54.
Carnell, R., 2012. LHS: Latin Hypercube Samples. . http://cran.r-project.org/package=lhs.
Cogley, J.G., 1999. Effective sample size for glacier mass balance. Geogr. Ann.: Ser. A Phys. Geogr. 81 (4), 497–507.
Cogley, J.G., Hock, R., Rasmussen, L.A., Arendt, A.A., Bauder, A., Braithwaite, R.J., Jansson, P., Kaser, G., Möller, M., Nicholson, L., et al., 2012. Glossary of glacier mass balance and related terms. Polar Rec. 48 (4), 1475–3057.
Cuffey, K.M., Paterson, W., 2010. The Physics of Glaciers. No. 4. Elsevier.
Dette, H., Kunert, J., Pepelyshev, A., 2008. Exact optimal designs for weighted least squares analysis with correlated errors. Stat. Sin. 18 (1), 135–154.
Fountain, A.G., Vecchia, A., 1999. How many stakes are required to measure the mass balance of a Glacier? Geogr. Ann.: Ser. A Phys. Geogr. 81 (4), 563–573.
Kiselák, J., Stehlík, M., 2008. Equidistant and D-optimal designs for parameters of Ornstein–Uhlenbeck process. Stat. Prob. Lett. 78 (12), 1388–1396.
Kuhn, M., 1984. Mass budget imbalances as criterion for a climatic classification of glaciers. Geogr. Ann.: Ser. A Phys. Geogr. 66 (3), 229–238.
Lliboutry, L., 1974. Multivariate statistical analysis of glacier annual balances. J. Glaciol. 13 (69), 371–392.
Müller, W., Stehlík, M., 2009. Issues in the optimal design of computer simulation experiments. Appl. Stoch. Models Bus. Ind. 25 (2), 163–177.
Näther, W., 1985. Effective Observation of Random Fields. Teubner Texte zur Mathematik.
Pázman, A., 2007. Criteria for optimal design of small-sample experiments with correlated observations. Kybernetika 43 (4), 453–462.
Rasmussen, L., Andreassen, L., 2005. Seasonal mass-balance gradients in Norway. J. Glaciol. 51 (175), 601–606.
Rempel, M.F., Zhou, J., 2014. On exact k-optimal designs minimizing the condition number. Commun. Stat. Theory Methods 43 (6), 1114–1131.
Rivera, A., Bown, F., Napoleoni, F., Mu noz, C., Vuille, M., 2016. Balance de masa glaciar. Ediciones CECs, Valdivia.
Rybicki, G., 1994. Notes on the Ornstein–Uhlenbeck Process. .
Smit, J.C., 1961. Estimation of the mean of a stationary stochastic process by equidistant observations. Trabajos de Estadística y de Investigación Operativa 12 (1), 35–45.
Stehlík, M., Aguirre, P., Girard, S., Jordanova, P., Kiselák, J., Torres, S., Sadovský, Z., Rivera, A., 2017. On ecosystems dynamics. Ecol. Complex. 29, 10–29.
Stehlík, M., Dušek, J., Kiselák, J., 2016. Missing chaos in global climate change data interpreting? Ecol. Complex. 25, 53–59.
Stehlík, M., Kiseľák, J., 2016. On stochastic representation of blow-ups for distributed parameter systems. Lect. Notes Comput. Syst. 132–140.
Stehlík, M., Rodríguez-Díaz, J.M., Müller, W.G., López-Fidalgo, J., 2008. Optimal allocation of bioassays in the case of parameterized covariance functions: an application to lung's retention of radioactive particles. Test 17 (1), 56–68.
Xia, G., Miranda, M.L., Gelfand, A.E., 2006. Approximately optimal spatial design approaches for environmental health data. Environmetrics 17 (4), 363–385.
Ye, J.J., Zhou, J., 2013. Minimizing the condition number to construct design points for polynomial regression models. SIAM J. Optim. 23 (1), 666–686.